Geohydrological modelling

Predictions for an area-oriented approach for groundwater contamination in the City of Utrecht

Investing in Opportunities
This project has received European Regional Development Funding through INTERREG IV B.
INTERREG IVB
Gemeente Utrecht
NL Agency
Ministry of Infrastructure and the Environment
Deltares
Enabling Delta Life

Summary

A geohydrological model has been developed in order to predict the behaviour of a number of plumes with chlorinated hydrocarbons in the city of Utrecht. The model is set up to support the area-oriented approach for groundwater contamination. As starting point, the model developed by Arcadis (Arcadis, 2009) has been used. It has been refined to layers of 0.5 m thickness and extended with an improved characterisation of the hydraulic conductivity by incorporating the recent developed GeoTOP. An improvement of the GeoTOP characterisation is under construction as numerous borehole descriptions gathered by the Municipality of Utrecht were not included in the original GeoTOP. A description of the workflow of this improved GeoTOP analysis is part of this report, but the final GeoTOP results are not yet available. They will be incorporated in future analysis.

Using the original GeoTOP data, the geohydrological flow model was run and a streamline analysis was performed for streamlines starting at the present plume locations. Most modelled streamlines end up in two large abstraction wells in the western part of the Municipality of Utrecht at 'Lage Weide' and near 'Leidsche Rijn'. The non-retarded travel times towards these wells are 115 to over 1000 years. The effect of preferential flow on the streamlines has also been analysed for four locations. Streamlines were started at different depths and it turned out that the travel times for a horizontal displacement of 1000 m could vary up to a factor 3 due to variations in hydraulic conductivity.

A reactive transport model based on streamline analysis has been applied. This model incorporates the sequential biodegradation of chlorinated hydrocarbons and retardation. Based on parallel research, the degradation of cisDCE in the model is assumed to be very slow or even not occurring at all. Therefore, model predictions show the development of long contaminant plumes that exceed the 'tussenwaarde' value, but do not reach the abstraction wells nor the border of the municipality within 200 years. In about 30% of the Monte Carlo runs, the concentrations at the front of the plumes are degraded to less than the 'tussenwaarde' value after 200 years, whereas in the other 70% of the Monte Carlo runs the norm is exceeded also at the front of the plume after 200 years.

When analysing the model in more detail and comparing them with available data, we recommend to improve the drainage levels in the city of Utrecht and to incorporate improved estimates of the biodegradation rates and validate the model by comparing plume predictions with the real world plume data. Moreover, additional data is foreseen to be used in the model: the improved GeoTOP results and improved characterisation of the present contamination. Finally the effect of ATES on the flow, the dispersion/mixing of contaminant and degradation rates should be included.

Table of content

1 Relation between this research and the conceptual site model (CSM) Utrecht

1.1 Introduction

The geohydrological flow and transport model is one of the research tasks addressed in the report of the conceptual site model. It has a strong link with the other research projects:

1. The volatilisation risk project will provide insight under which circumstances risk of vapour intrusion exists and how relevant processes attenuate these risks. The geohydrological flow and transport model calculates areas where contaminant plumes gets near the surface, including estimates of concentrations. In combination with the outcome of the volatilisation risk project, areas with increased risk for vapour intrusion can be determined and used for the design of a monitoring strategy for the area-oriented approach.
2. The flux determination project will determine the amount of flux that is dissolved in source zones. The outcome of this project will be used to validate the calculated water and mass flux in the geohydrological model and if needed the model can be updated.
3. The biological degradation capacity project will determine the relevant biodegradation pathways and supply biodegradation rates for it. Preliminary results have been translated into the biodegradation rates used by the transport model and more final results should be used to get the best model predictions.
4. The 'impact of ATES' project, when started, can make use of the model and predict the behaviour of contamination near an ATES system. Using additional monitoring data , this project can determine and quantify the relevant processes and if necessary additional processes can be included in the geohydrological model

In combination with these other projects the geohydrological model will help to determine:

1. the boundaries of the area-oriented approach;
2. the impact of the contamination on receptors (including vapour intrusion);
3. a spatial distribution of the probabilities where plumes may pass the boundary of the area-oriented approach at unacceptable concentrations, that is to be used for the design of a monitoring strategy and fall back scenario's;
4. remediation targets for present plumes that threaten to pass the boundaries with unacceptable concentrations.

1.2 Present status

The geohydrological model has not been finalized due to time constraints of the CityChlor project. Therefore, some of the present results will be improved in the near future. This will be addressed in the text.

2 Geological model

In this chapter the geological description, the geological model GeoTOP and the groundwater flow model is introduced. Both models provide input to the reactive transport model that is described in chapter 3.

2.1 Geological description

2.1.1 Description of heterogeneity

The subsurface of the City of Utrecht is known to be heterogeneous. In general, it is characterized by two main aquifers at approximately - 5 m to -45 m +NAP and -70 m to -110 m +NAP. However, throughout the subsurface of the city of Utrecht various river channel deposits of the Rhine river system have been deposited which at some places results in a direct connection between the two main aquifers. The channel deposit of the Rhine river also shows a strong spatial variation, which altogether results in a heterogeneous subsurface. This can be clearly seen in the borehole data that is present in database DINO (www.dinoloket.nl). Figure 2.1 shows borehole description in a north-south oriented cross-section in the city of Utrecht.

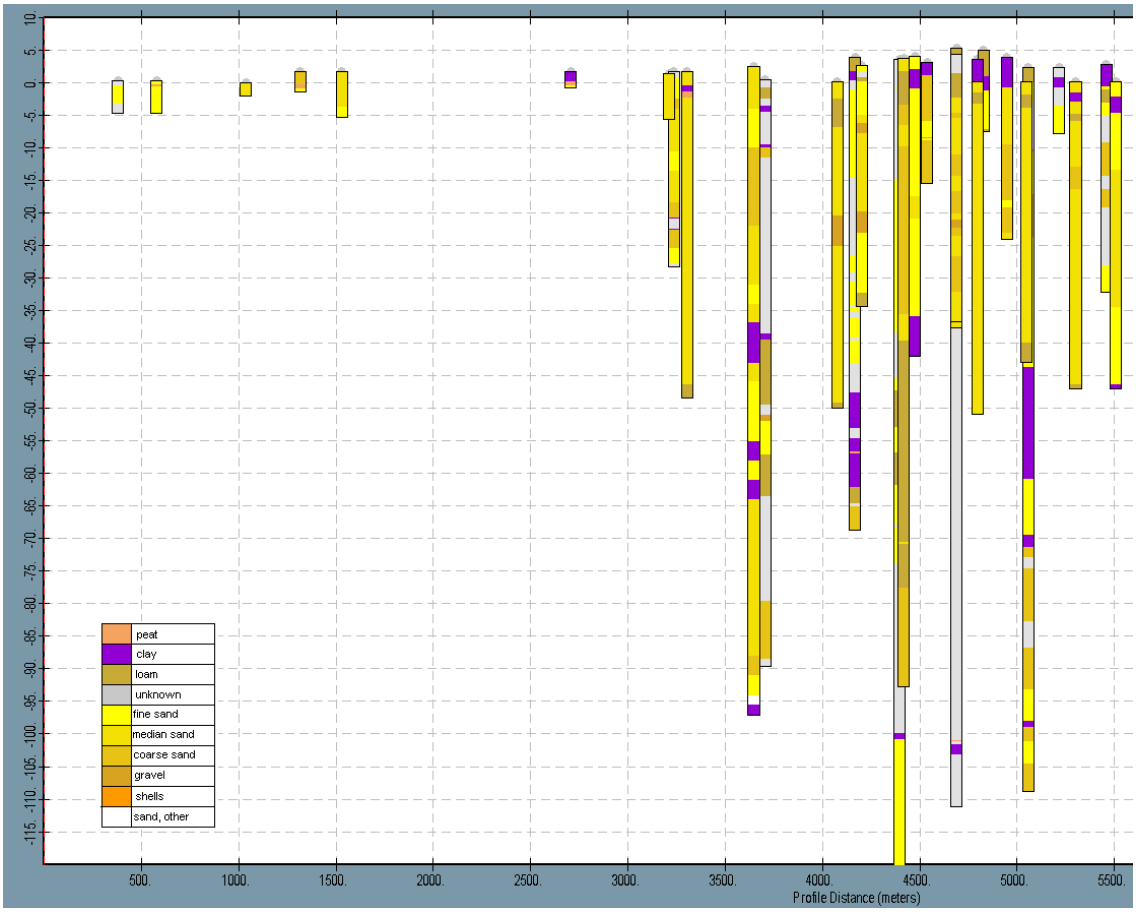

Figure 2.1 North (left)-South(right) cross-section with borehole description data with lateral offset of 100 m

In this cross section, it is clear that at -40 to -70 m +NAP a clay layer is present, but in some boreholes this clay layer is absent and the levels at which clay is observed can strongly vary over a short distance. Moreover, the sandy layer above is not homogeneous: borehole descriptions vary from fine sand to gravel.

2.1.2 GEOTOP model input

The heterogeneity of the subsurface of all regions in the Netherlands is or will be represented using the voxel model GEOTOP. This model consists of voxels (model cells) of 100 m x 100 m x 0.5 m in each of which the lithology and horizontal and vertical hydraulic conductivity is estimated. The depth of this GEOTOP model varies between regions. For the city of Utrecht and vicinity the GEOTOP model extends to a depth of -50 m +NAP.

TNO recently introduced this geological model which is available via the webportal DINOLOKET (www.dinoloket.nl). Unfortunately, a large dataset of borehole descriptions for the municipality of Utrecht was not incorporated when TNO made this GEOTOP model for this region. These data were not registered on time in the database DINO, that TNO used as a starting point. TNO performed additional work to incorporate these new borehole descriptions and recalculated the GEOTOP for this project.

In short, the GEOTOP model is based on the following workflow:

1 The boundaries of different geological formations are determined.

2 A geostatistical analysis of the lithologies (such as clay, sand, loam, etc.) within each geological unit is performed using the available borehole data.

3 For all voxel cells of 100 m by 100 m by 0.5 m, stochastic realisations are obtained for the lithology, based on the geostatistical data of the geological formation and conditioned on the borehole data. This action is repeated 100 times, so 100 equal likely realisations of the lithology in the subsurface are obtained.

4 Using these 100 realisations, the probability of each lithology in each voxel cell is calculated and the most likely lithology is calculated.

5 Finally, the lithology is translated into horizontal and vertical hydraulic conductivities for the most likely lithology (original GEOTOP approach) or also for all realisations (on request for this project).

In appendix A shows a more details description of this analysis.

An example of the cross section of the horizontal hydraulic conductivity is given in

Figure **2.2**.

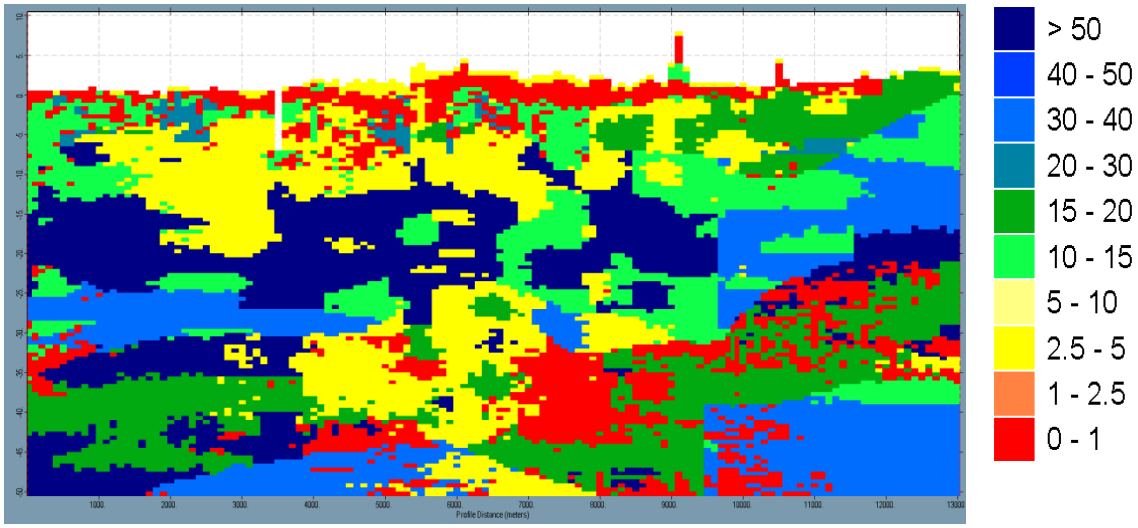

Figure 2.2 Example of a cross section of hydraulic conductivity (m/day) (original GEOTOP model)

In this cross section, it is clear that there is a strong variability in the hydraulic conductivity, with regions with for instance hydraulic conductivity of over 50 m/day below regions with a conductivity of less than 5 m/day. Originally, both such regions were classified in the same aquifer often with an equal hydraulic conductivity. For contaminant transport, it is to be expected that this variability will lead to preferential flow.

The total data set of this GEOTOP model is a large 3 dimensional dataset with 100 equally likely realisations.

2.2 Groundwater flow model

History of the groundwater flow model

The groundwater flow model is based on the groundwater flow model of Arcadis (Arcadis 2009). The horizontal extension of the model is shown in Figure 2.3.

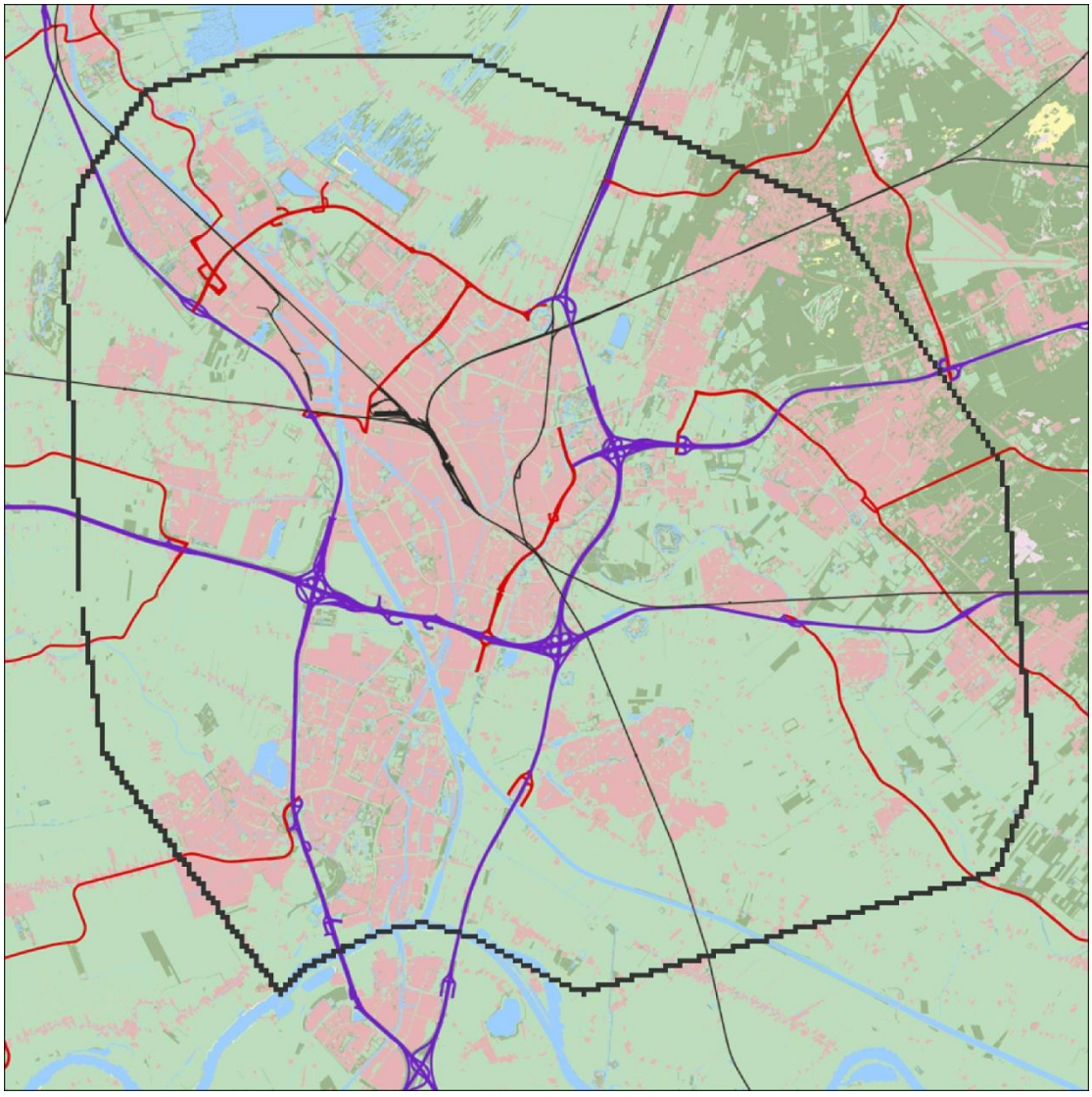

Figure 2.3 Extension of the groundwater model, purple lines are motorways, red lines are other main roads and thin black lines are railways

It has been refined in the vertical direction so that the layer thickness has become 0.5 m for all layers at which the GEOTOP has been analysed (until -50 m +NAP). Below, the original layer tops and bottoms of the Arcadis model are used for 5 model layers. The vertical position of all relevant items (such as abstraction wells, rivers boundary conditions, etc.) were obtained from the layer(s) of the original model and distributed over a number of layers of the new schematisation. In total, the model consists of 126 model layers.

2.2.1 General description of the geohydrological system

The groundwater flow in the vicinity of the city of Utrecht is dominated by a few physical boundaries. East of the city of Utrecht a large infiltration area, 'The Utrechtse Heuvelrug' is present. The area west and north of the city of Utrecht consist of polders where surface water levels are kept low and which act as seepage areas. On the regional scale, the groundwater flows from 'The Utrechtse Heuvelrug' underneath the city of Utrecht towards the polders north and west of the city of Utrecht. This is schematised in Figure 2.4.

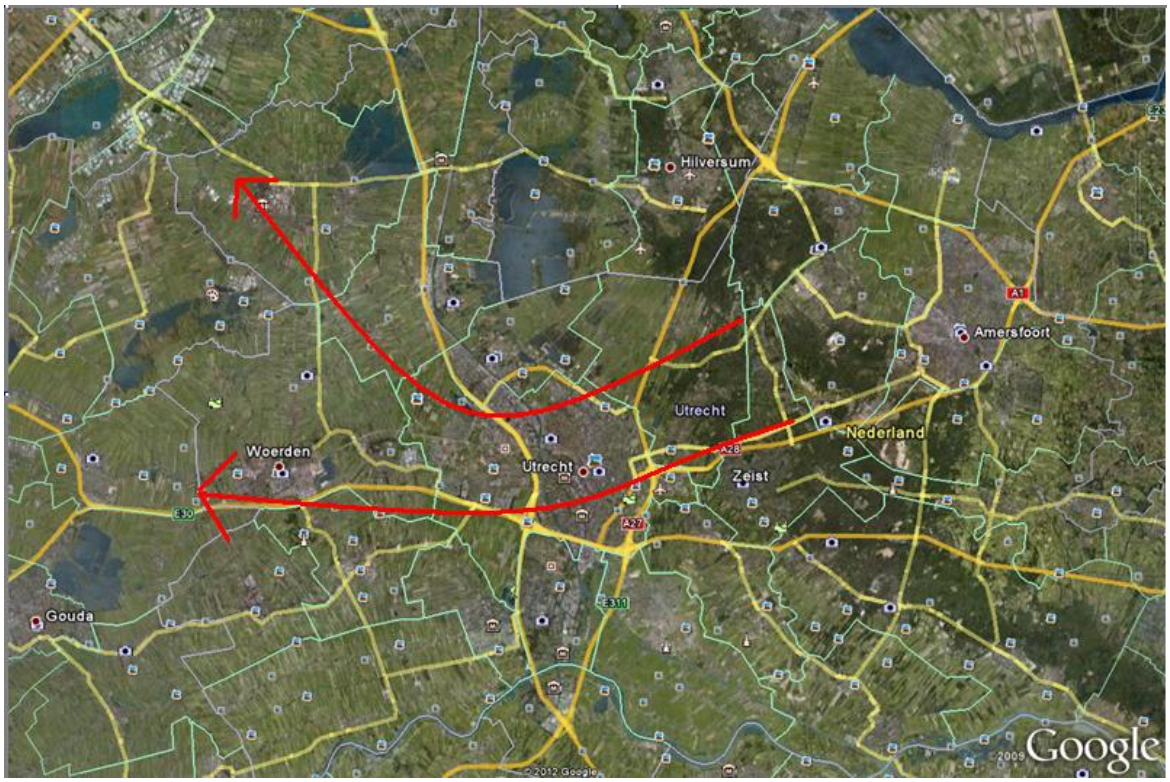

Figure 2.4 Regional pattern of groundwater flow

The model does not fully contain the infiltration and seepage area, but their influence is modelled by imposing constant head boundary conditions at the boundaries of the model domain.

Within the city of Utrecht some local aspects does influence the groundwater flow, such as groundwater abstraction wells and ATES system. Moreover, the water table in the confining top-layer is influenced by local surface water and drainage systems.

The following model results are without the ATES systems in this area, as the reactive transport model described in the next chapter needs to be extended to incorporate the effect of transient groundwater flow. Furthermore the influence of the mixing of ATES systems on biodegradation rates is not yet quantified. Moreover, the up to date data of the ATES systems was not available. The municipality of Utrecht provided a new data set with many more ATES systems than incorporated in the model by Arcadis. At this moment, xy-locations for the individual wells of the ATES systems are lacking.

2.3 Groundwater model results

The stationary hydraulic heads that are obtained for the groundwater flow model, with the most likely GEOTOP data, are shown for the model layer at - 20m + NAP in Figure 2.5.

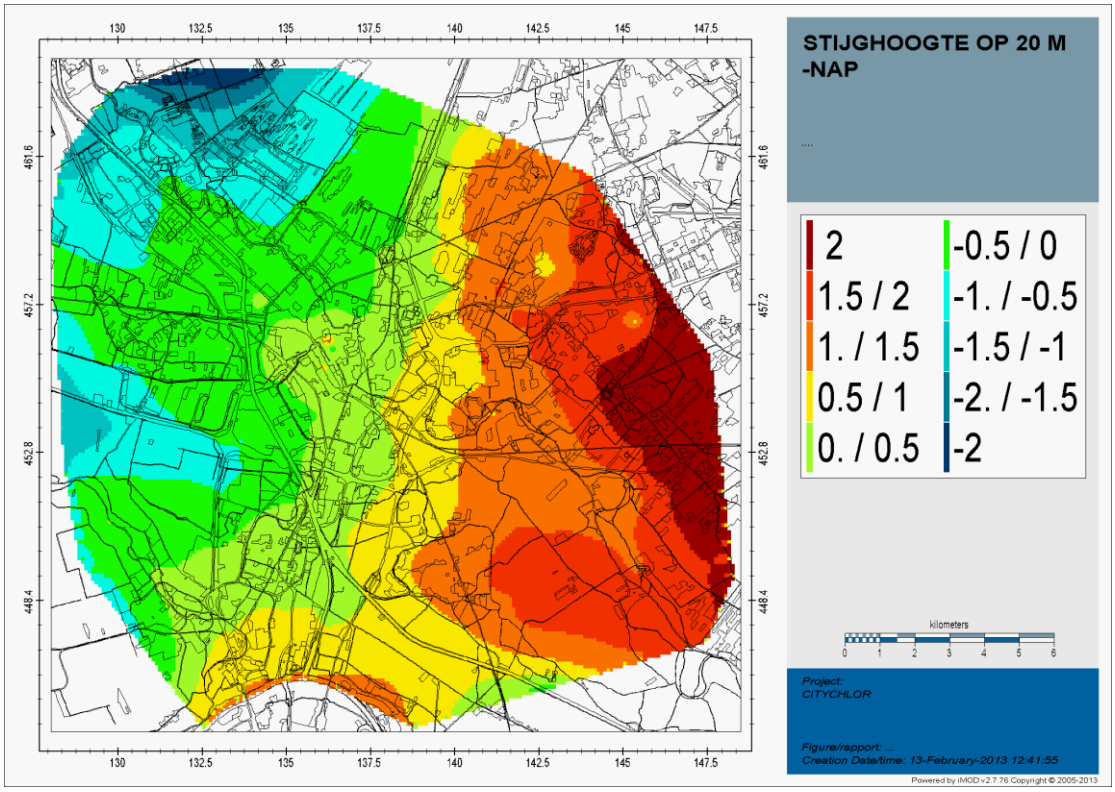

Figure 2.5 Simulated hydraulic heads at -20 m + NAP

Pathlines calculations were performed with starting locations at contaminated areas. These contaminated areas are chosen equal to the initial contaminant situation that was identified by Arcadis (2009). This initial contaminant situation is shown in

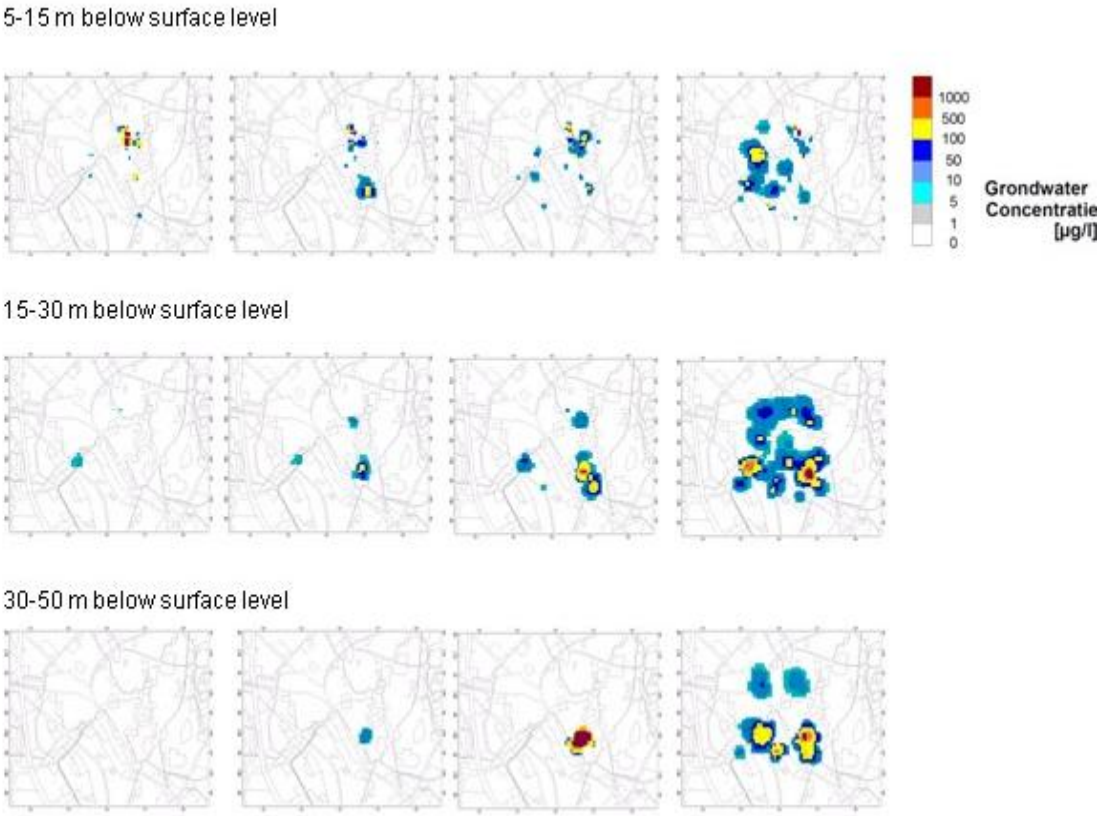
5-15 m below surface level
1000
500
100
50
10
5
1
0
Grondwater
Concentratie
[µg/l]
15-30 m below surface level
30-50 m below surface level

Figure 2.6.

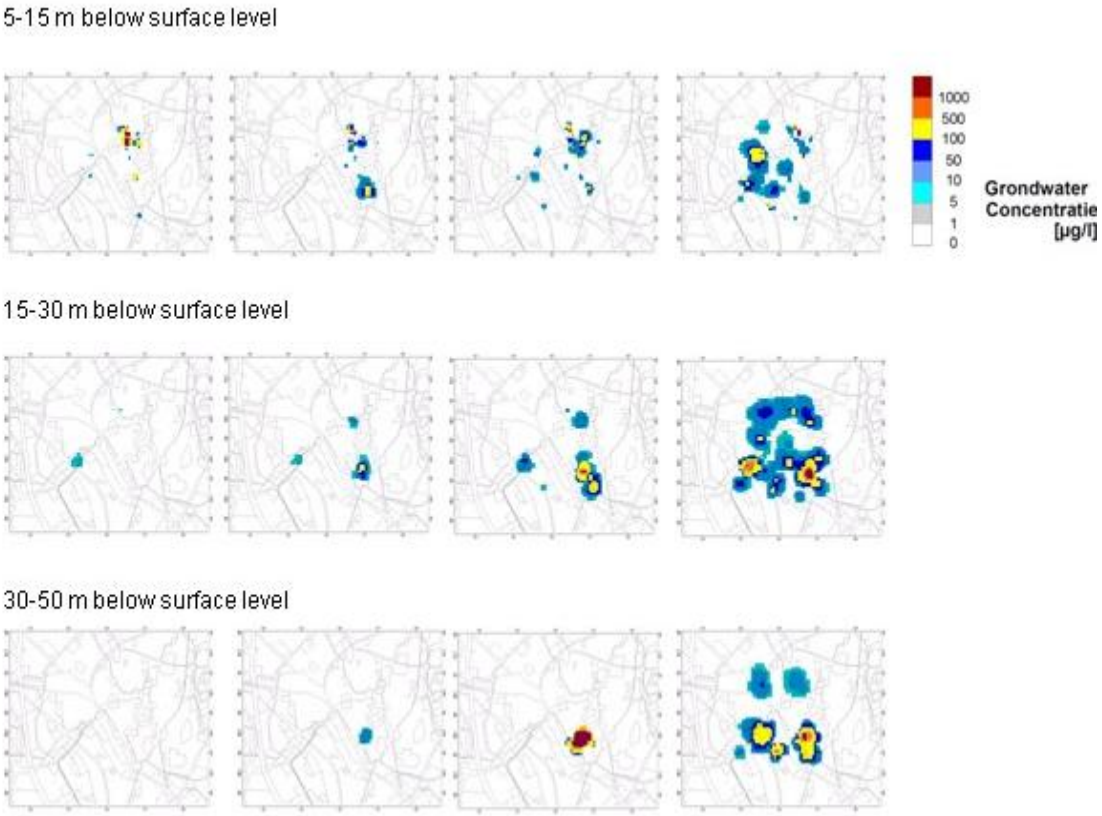

Figure 2.6 Initial situation of contamination that is used as starting locations of streamlines; from left to right: PCE, TCE, cisDCE and VC

From this figure, it is clear that the highest concentrations of cisDCE and VC are encountered in the deeper layers. It is expected that this depiction of the contaminant situation is not complete and that there are more contaminant plumes; the municipality of Utrecht is working on gathering a new data set. This new data set will be incorporated in future calculations.

In the Arcadis model, the plumes were defined in 3 model layers of 15 m thickness model, pathlines start at each layer of 0.5 m thickness. The simulated streamlines are shown in

Figure 2.7.

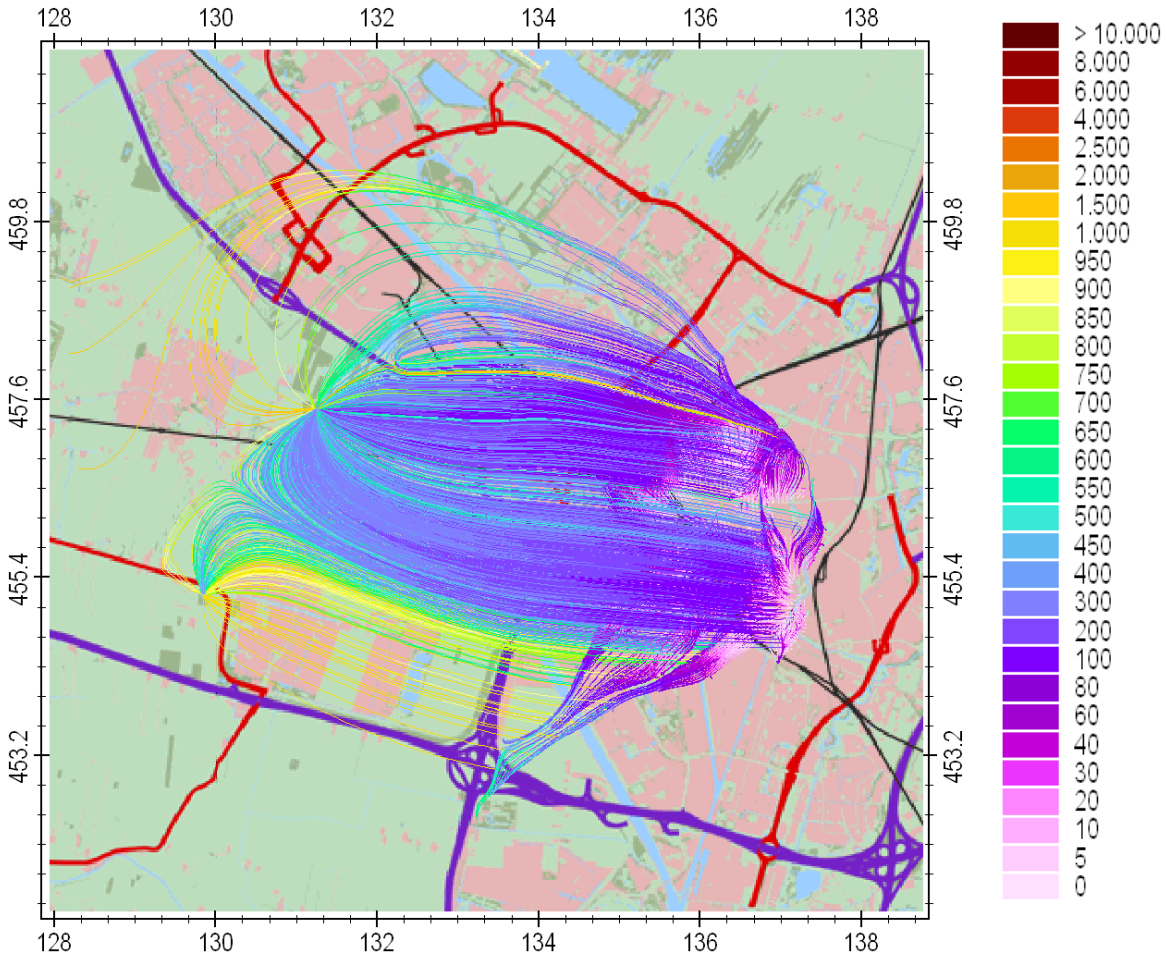

Figure 2.7 Pathlines starting at initial contaminant plumes (colour legend denotes conservative travel time in years)

It shows that most pathlines finally end in two abstraction wells; one at Lage Weide and one just west of Leidsche Rijn. The travel times are at least 115 years, but travel times of over 1000 years also occur.

In order to show the depth at which these pathlines are located a selection of these pathlines (starting at depths -10, -22.5 and -40 m +NAP) are plotted in the three dimensional Figure 2.8.

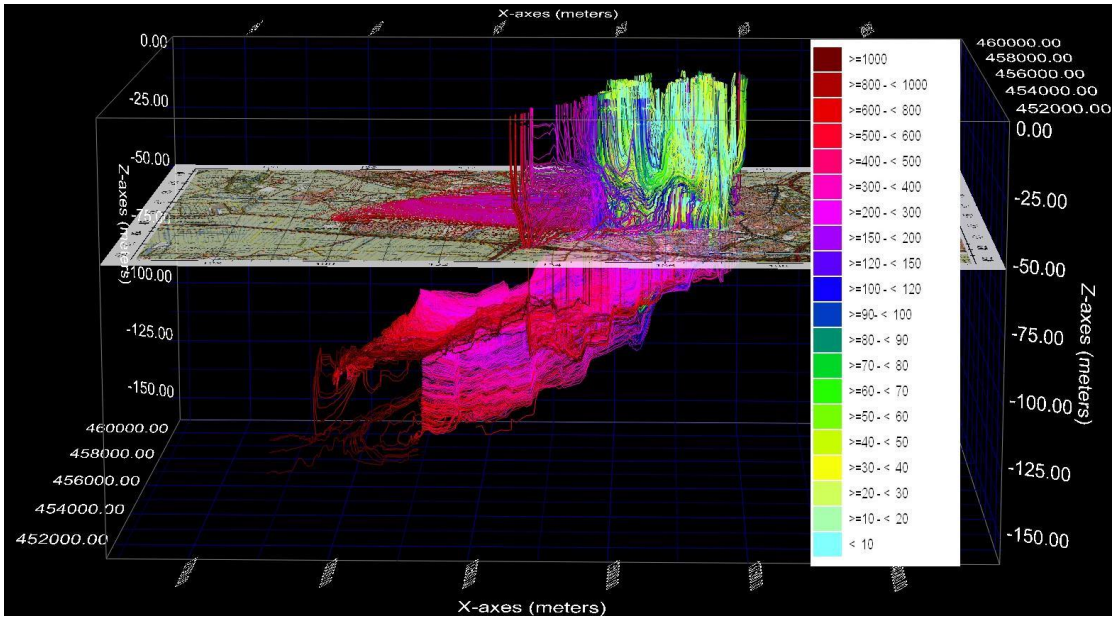

Figure 2.8 3D figure of pathlines starting at depths -10, -22.5 and -40 m +NAP; colours denote conservative travel time in years; the topography is plotted on the depth of -50m +NAP with pathline below this depth are also projected on the topography

Within the GeoTOP extension (above -50 m +NAP), the pathlines show a strong vertical flow. Pathlines either go upward towards a seepage boundary conditions or go downward until they reaches the first aquifer below the GeoTOP extension and then go more horizontal in western direction. Both pathline patterns need some additional attention. The drainage levels in the city in the original model of Arcadis are sometimes lower than commonly expected. Also, the effect of incorporating the GeoTOP above -50 m NAP in the model should not result in a too strong reduction of the effective hydraulic conductivity of the aquifers that fall within the GeoTOP, with the result the a larger portion of the groundwater flows through the deeper aquifers. Both aspects will be analysed critically and if needed the model will be updated in the near future.

In order to analyse the occurrence of preferential flow, arrival times for a horizontal flow displacement of 1000 m within the GeoTOP layers were analysed. They were started at the same xy-location but at different depths for four xy-locations. The results are shown in Figure 2.9.

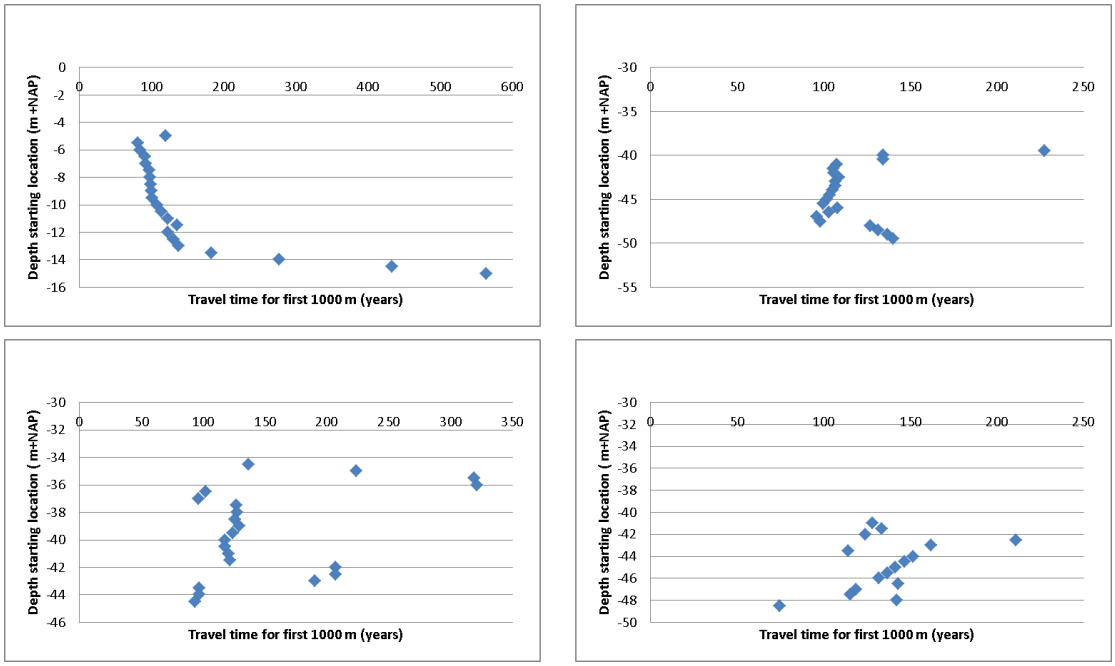

Figure 2.9 Travel times for first 1000 m for particles starting at four locations as function of starting depth

In the first figure, the travel time gradually increases with increasing depth with a strong increase for starting locations between -13 and -15 m +NAP. These streamlines enter a less permeable zone at greater depth, which results in larger travel times. The second figure shows deviating travel times for the upper and lower starting locations. The last two figures show strong variation in travel times up to a factor 3 for starting locations also in the middle of the plume depths. The variation in hydraulic conductivity as present in the GeoTOP dataset results in strong variation in plume displacement and travel times. The original model used a uniform hydraulic conductivity distribution for the depths at which this analysis was performed. The present model also predicts early arrival times at control planes due to preferential flow. Moreover, the effect of biodegradation could be overestimated when preferential flow is not incorporated in the geohydrological model: the time at which biodegradation is presumed to take place before arriving at a control plane would be overestimated.

3 Reactive transport model

3.1 Introduction

Standard groundwater contaminant transport models, such as MT3D or RT3D would require an enormous calculation time, when applied at the scale of a large city with a vertical discretization (cell size) of 0.5 m in the vertical direction. These models are commonly applied for the calculation of a single plume at site scale. Deltares has developed an alternative approach and has also applied it for the area-oriented approach for the Port of Rotterdam (Marsman et al., 2005). This alternative approach has been used in the Citychlor project.

3.2 Method

3.2.1 Arrival time

This approach consists of calculation of transport and biodegradation along streamlines. For all model cells at source zones and present plumes, pathlines were calculated. Initial concentrations for all components are given to each streamline at the start. These concentrations are based on the dissolved concentration estimates derived from field data. It is assumed that the measured field data are the result of a pure liquid phase source and that concentrations at the source zone remain constant. Next, the concentrations and the arrival time are calculated by following the streamline. The time at the start of the streamline is chosen to be 2009, (the year at which the initial contamination situation was analysed). In each model cell along the pathline the residence time of each component is added to obtain the component's arrival time in the next cell along the pathline. The component's residence time in each model cell is obtained by multiplying the conservative residence time with the retardation factor of that component.

3.2.2 Biodegradation reactions

The following biodegradation reactions are modelled:

- *Reductive dechlorination*

PCE →TCE → cisDCE → VC→ harmless product

- *Oxidative degradation*

cisDCE→ harmless product

VC→ harmless product

All reactions are modelled as first order degradation where the degradation rate may depend on the redox or contaminant condition of the model cell.

$$C = C(0)\exp(-k \bullet dt)$$

with *C* is the component's concentration when leaving the model cell [µg/l]; *C(0)* is the concentration at the entrance of the model cell [µg/l]; *k* is the first-order biodegradation rate [day^{-1}], and *dt* is the residence time of the component in the water phase of that cell [day].

For the sequential degradation, the concentration of one component that is degraded is added to the next component taking into account the stoichiometric ratio: the ratio of the mass of one component that is produced and the mass of the mother component that is consumed.

3.3 Potential control planes

For the potential control plane, it was decided to choose the municipality border. However, a small area of the municipality of Utrecht falls outside the model domain. For that area the boundary of the model was chosen as the potential control plane. When arriving at the control plane, concentration estimates of each streamlines are compared with the 'Tussenwaarde'-norm, see

Table 3.1. If in a model cell, the concentration of one of more components exceeds this norm and has an arrival time that is smaller than the time of interest, it is recorded that the norm is violated in that model cell at the time of interest.

Table 3.1 'Tussenwaarden'-norm for the CHC-components

CHC-component	'Tussenwaarde'-norm (µg/l)
PCE	20.005
TCE	262.0
cisDCE	10.005
VC	2.505

The total results of all streamlines will give an indication where and from when on unacceptable breakthrough can take place. Moreover by performing a Monte Carlo analysis, the chance of an unacceptable breakthrough at those locations is obtained as well. It turned out that the contaminants did not reach the municipality border within 200 years and therefore for breakthrough results were plotted for the entire model domain and not only at the potential plane of compliance.

3.4 Motivation for negligence of several processes

This approach of calculation of transport along streamlines neglects or simplifies a number of processes that are justified below.

- Dissolution at source zones with constant concentrations.

The dissolution of the CHC (chlorinated hydrocarbons) contaminants at source zones is a process that is hard to quantify in practice. In general, CHC components have been spilt into the subsurface as pure phase (DNAPL) and due to its high density, they have sunk into the subsurface. Less permeable layers can act as a barrier for the DNAPL, but when the DNAPL builds up a high enough pressure it may overcome the capillary pressures and flow through the barrier. At the entire pathway of the DNAPL, a pure phase will remain behind in the larger pores (residual) and as pools on less permeable layers. Both pools and residual DNAPL will act as long term source for dissolved groundwater contamination. In practice, we often only encounter the result of this dissolution process by taking and analysing groundwater samples at a number of monitoring wells near the source zones. Thus although we cannot quantify the dissolution processes, we have information about the final result of the dissolution process, namely the concentration values in the groundwater near the source zones. By assuming in the model that these concentration remain constant in time in time, we neglect the possibility that source zone may (partially) dry up. This is, however, a conservative assumption: in reality dissolved concentrations in source zone areas might become lower when the source zone starts to dry up, but generally this drying up process may take decades or even centuries. Moreover, the model results are used to predict whether a plume may pass a control plane at unacceptable levels and if needed additional monitoring at this boundary will be performed.

- Dispersion/diffusion

The negligence of dispersion and diffusion is also a conservative assumption. In reality, both processes will result in decreasing peak concentrations. Consequently, the model may thus overestimate the maximum concentration of the plume at arrival at a control plane. The model may underestimate the width and thickness of the plume by neglecting dispersion and diffusion in the transversal direction and may overestimate the arrival time by neglecting dispersion and diffusion in the longitudinal direction. The latter should be taken into account when designing a monitoring strategy when unacceptable concentrations are expected to pass a control plane.

The underestimation of the width and the thickness of a plume at a control plane is dealt with by monitoring at a control plane. When it reports that an unacceptable concentration passes the control plane, additional monitoring in the width and the thickness of the plume is needed in order to design a proper fall back scenario.

The underestimation of the plume thickness when a plume approaches the water table should be taken into account when quantifying the risk for vapour intrusion. Based on the length of the streamline and the transversal dispersivity and/or the residence time and diffusion coefficient the increased thickness of the plume with concentration profile near the water table can be estimated. This needs be worked out.

- Effect of consumption of redox components by contaminant degradation

The effect of biodegradation on the consumption of redox component is relevant for the oxidative biodegradation as with this reaction the redox component oxygen is consumed. For microaerophilic oxidative degradation the amount of oxygen present is limited and the oxygen could in reality be depleted before all VC and cisDCE is degraded oxidatively. The model code could easily be extended that only a limited amount of oxygen is present and that oxidative degradation stops after a certain amount of oxygen has been consumed following a pathline. In the present model runs, it was assumed that the amount of oxygen is not limiting, but in future runs a maximum amount of degradation of VC and cisDCE along a pathline will be incorporated. For reductive dechlorination, the effect of the degradation on the redox component is assumed to be negligible.

3.5 Input data

Retardation

A value of 0.1% of organic matter was used for the entire model domain in order to simulate retardation. This values was taken equal to the values applied by Arcadis (Arcadis 2009). It results in the following retardation factors: 1.8 for pCE; 1.4 for TCE; 1.2 for cisDCE, 1.1 for VC.

Biodegradation rates

The biodegradation is quantified in a parallel research project within the Citychlor program. This research had not been finalized at the time the model calculations were performed and the results did show a large variation. Based on oral and email communication with Shakti Lieten (Bioclear) and some additional data interpretation, the following biodegradation rates were used.

- Reductive dechlorination

  The reductive dechlorination of PCE and TCE seems to be a fast process. The initial condition of the Arcadis model (Arcadis, 2009, figure 4.1) confirms this trend as the initial PCE and TCE concentrations, derived from field data, predominantly show some small hotspots without large plumes. In contrary, initial DCE and VC concentrations show more extensive plumes. It suggests that PCE and TCE, when dissolved at a DNAPL source area, degrade relatively quickly compared to DCE and VC.

  For the reductive dechlorination of PCE and TCE a first order biodegradation rate of 0.05 day^{-1} is used in the model.

  For the reductive dechlorination of DCE, Bioclear derived values of 0.05 day^{-1} in cases with high CHC concentrations, whereas in plumes with low CHC concentrations no biodegradation was observed in a majority of the well and in other wells biodegradation rates ranged from 0.001 day^{-1} to 0.0001 day^{-1}.

  In the model, the following biodegradation rates for DCE and VC are used:

  If the total CHC concentration exceeds 1000 µg/l: a first order reductive biodegradation rate of 0.05 day^{-1} is used.

  If the total CHC concentration is less than 1000 µg/l the first order reductive biodegradation rate of DCE and VC is considered as a stochastic variable. It is assumed to have a 70% chance to be 0 and the remaining 30% are uniformly distributed between 0.001 day^{-1} and 0.0001 day^{-1}.

For each Monte Carlo run, only a single value is drawn for the reductive dechlorination rates of DCE and VC and is applied for all plumes. In reality, it may be possible that a plume encounters areas with no biodegradation and more downgradient it travels through an area with more favourable conditions with non-zero biodegradation rates. However, we propose at this moment to use the conservative assumption that reductive dechlorination may not take place for the entire pathway.

- Microaerophilic degradation

  DCE and VC are known to be able to be oxidized under low oxygen concentrations. In the parallel study micro-aerophilic degradation of VC was observed in a large number of wells, whereas microaerophilic degradation of DCE was observed in only a small percentage of the wells.

  In the model, a value of 0.02 day^{-1} is used for the first order oxidative degradation of VC (based on the minimal value for VC oxidation under the hypoxic conditions, in USGS, 2012). For DCE, this value is taken as zero.

3.6 Model results

As a part of the model input parameters are stochastic variables, so is the model output. In order to calculate the model output, including its uncertainty, a Monte Carlo analysis is performed: the stochastic model is run, by drawing randomly from the probability density function of the stochastic model input parameters; next the model is run and the relevant results are stored after some post-processing. By repeating this workflow a hundred times, hundred possible outcomes for the model results are obtained and they can be used to derive a probability density function for the model results.

It is very difficult to visualize the outcome of these stochastic 3D model output directly. Therefore, the model results are summarized as follows: For a number of times, it is checked if any of the components PCE, TCE, cis-DCE or VC exceeds the 'tussenwaarde'-norm in each model cell for a Monte Carlo realisation. This gives a 3D data set where the norm is exceeded for at least one component. Next, this 3D data set is summarized by mapping this data set on a horizontal plane: so if in any layer the norm is exceeded it is recorded for the cell with the same horizontal coordinates. Finally, this workflow is repeated for the 100 Monte Carlo realizations and the result is summed. After division by 100 (the number of realizations) a top plane view is obtained that denotes the chance that in any cell in at least one layer, the norm is exceeded for at least one component at the specified time.

For January 1, 2043 the result is shown in Figure 3.1.

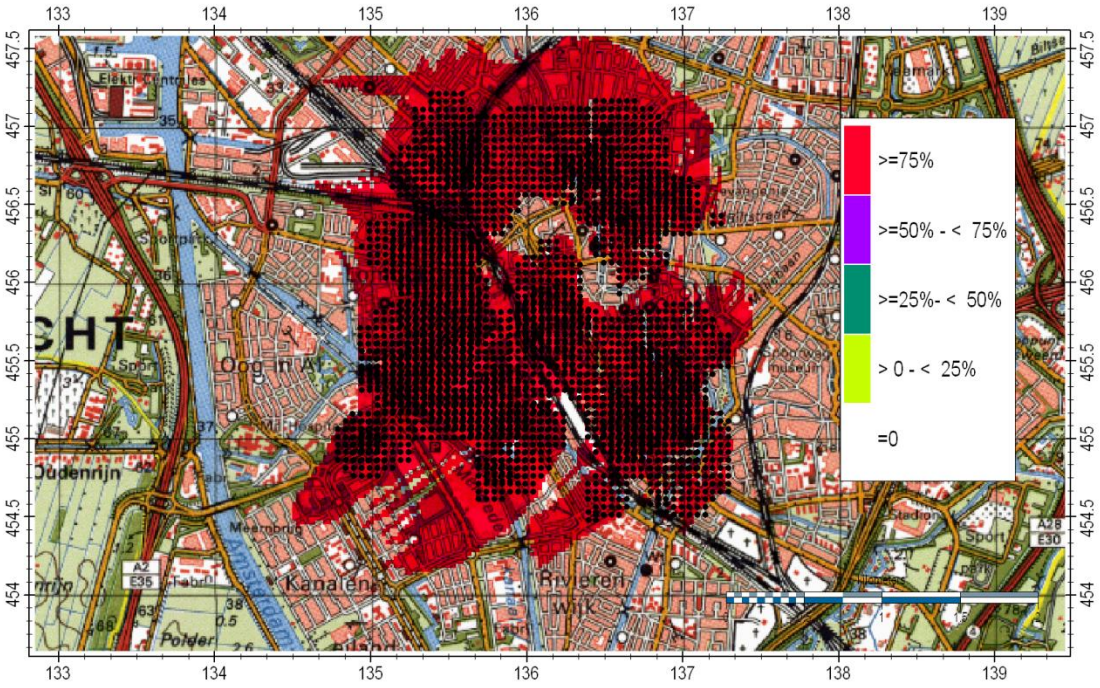

Figure 3.1 Top view with probability if the norm is violated for at least one component at 1-1 2043; black dots denote initial plumes

For other times the results are shown in appendix B.

3.7 Discussion

The streamlines show a typical behaviour. Initially the streamlines starting at the northern part of the city centre show a northern flow direction, whereas the streamlines starting at the southwest of the city centre show a south-western flow direction. Around and after 2043 part of the streamlines start to go in western direction. When analysing the streamlines, it turned out that this shift in flow direction coincides with the arrival at the model layers below the bottom of the GEOTOP at -50 m +NAP. Moreover, many streamline flow quickly in upward direction until they are close to the surface area and stop in a drainage cell. It turns out that the drainage levels in the model as were obtained from the Arcadis model are (too) low. It is strongly recommended to compare the modelled hydraulic heads with real world data and adapt the model when applicable. It is also remarkable that the contaminants have not reached the abstraction wells in the western part of the model yet after 200 years. Finally, it is clear that biodegradation rates in the present model are too low in order to prevent a significant spreading. Especially the degradation rate for cisDCE is responsible as it has a 70% chance to have a value of 0 and in the other 30% it has a simulated value between 0.001 and 0.0001 day^{-1} . Therefore for these 30%, cisDCE needs to be in dissolved phase between 2.7 to 27 years in order to have its concentration be reduced by a factor e (=2.718). Only in the figure B6 in Appendix **B**, some probability values at the front of the plume gets lower than 75%, meaning that in a number of Monte Carlo runs, degradation reduces part of the contamination below the 'Tussenwaarde'-norm.

Another aspect that needs attention in the model input are the biodegradation rates, especially for cisDCE and VC. In the present model setup, the biodegradation rate for cisDCE is zero in plumes with summed CHC concentrations lower than 1000 µg/l for 70% of the Monte Carlo runs. Therefore, most modelled plumes will predominantly consist of cisDCE. When analysing the initial concentrations, see Figure 2.6, that are derived from real world data, it is obvious that for most real world plumes, VC is more dominantly present than cisDCE. If VC is not the source contamination, the real world concentration data give an indication that cisDCE is degraded better than assumed by the model and/or VC degradation may be overestimated.

When comparing the present model results with the transport calculations described by Arcadis (2009), a remarkable difference can be observed. Arcadis reports that the clay layer between the first and the second aquifer prevents flow to the second aquifer. They report a vertical resistance of 4000 days, although in their model the value of the vertical resistance of the clay layer varies and values of less than 500 days can be found in the northern part of the city centre. Moreover, at some areas including the northern part of the city centre, the clay layer is entirely located above -50 m + NAP. On these locations the clay layer is replaced by the GeoTOP data in the improved model and although lower hydraulic conductivity values are simulated in this area, the pathlines go straight towards the second aquifer. Moreover, pathlines also reach the second aquifer in areas where the original resistance of the clay layer is taken over from the Arcadis model in cases were this layer was situated below -50 m + NAP (for instance south of the city centre). As Arcadis used relatively high biodegradation rates the development of plumes in the second aquifer was probably underestimated in their model.

Additional data output will be available in digital form, such as the full 3D data set with probabilities, maximum concentrations and arrival times for the four components, etc. With this data for instance it can be analysed where a norm is expected to be exceeded at a control plane, at what depths, for which components and which concentrations and at which time point.

4 Future plans

In the near future the following actions are recommended:

1. Improvement of model data and processes in the model
   - New GeoTOP dataset
   - Incorporate effect of ATES systems on mixing and degradation
   - Incorporated up to date contamination data
   - Improved biodegradation rates
   - Analysis and if needed update of drainage levels

2. Validation of the model with hydraulic head data and mass flux and plume flow direction data

3. Design monitoring strategy and fall back scenario

4. If needed, design preventive remediation targets for critical plumes.

5 Bibliography

01. Arcadis, Saneringsplan ondergrond Utrecht gefaseerde gebiedsgerichte aanpak; Arcadis report nr B02034/WA9/010/000055/001B/lm, 2009

02. Berendsen, H.J.A., & Stouthamer, E.,. Palaeogeographic development of the Rhine-Meuse delta, The Netherlands. Van Gorcum, Assen, 268 p., 2001

03. Chilès, J-P. & Delfiner, P., Geostatistics – Modeling Spatial Uncertainty. Wiley & Sons, Hoboken, New Jersey, 699 p., 2012

04. Goovaerts, P., Geostatistics for Natural Resources Evaluation. Oxford University Press, New York, 483 p., 1997

05. Marsman, A. , Valstar, J. & ter Meer, J. , Risk analysis on groundwater contamination at the megasite Port of Rotterdam, In: M.F.P. Bierkens, J.C. Gehrels & K. Kovar (eds.), Calibration and Reliability in Groundwater Modelling: From Uncertainty to Decision Making, Proceedings of ModelCARE 2005

06. Stafleu, J., Maljers, D., Busschers, F.S., Gunnink, J.L., Schokker, J., Dambrink, R.M., Hummelman, H.J., Schijf, M.L., GeoTOP modellering. TNO-rapport TNO 2012 R10991, 216 p., 2012

07. USGS, Microbial mineralization of cis-dichloroethene and vinylchloride as a component of natural attenuation of chloroethene contaminants under conditions identified in the field as anoxic. USGS Scientific Investigations report 2012-45032, 2012, http://www.clu-in.org/download/contaminantfocus/dnapl/Treatment_Technologies/Microbial-Mineralization-USGS-2012.pdf

Appendix A: Gemeente Utrecht - GeoTOP

For this study the GeoTOP workflow is followed, this workflow is presented in short in this report. For a full description of all actions see Stafleu et al. (2012).

Data preparation

Data used for this study has two sources, the DINO database and the Utrecht University borehole database, including the boreholes made for the mapping of the peat distribution in the province of Utrecht.

During the process of data preparation the descriptions of the new boreholes (delivered by the Gemeente Utrecht to DINO) have been checked on their consistency with regard to the data used in the GeoTOP Rivierengebied study. This consistency check consisted of a check of the data quality, of the geological interpretation of these boreholes and whether these boreholes have an influence on the geological concepts used.

In total 879 more boreholes have been used in this area than in the GeoTOP Rivierengebied study, the number of cone penetration tests ,used for the labeling of the Basisveen Bed, is unchanged (Figure A1).

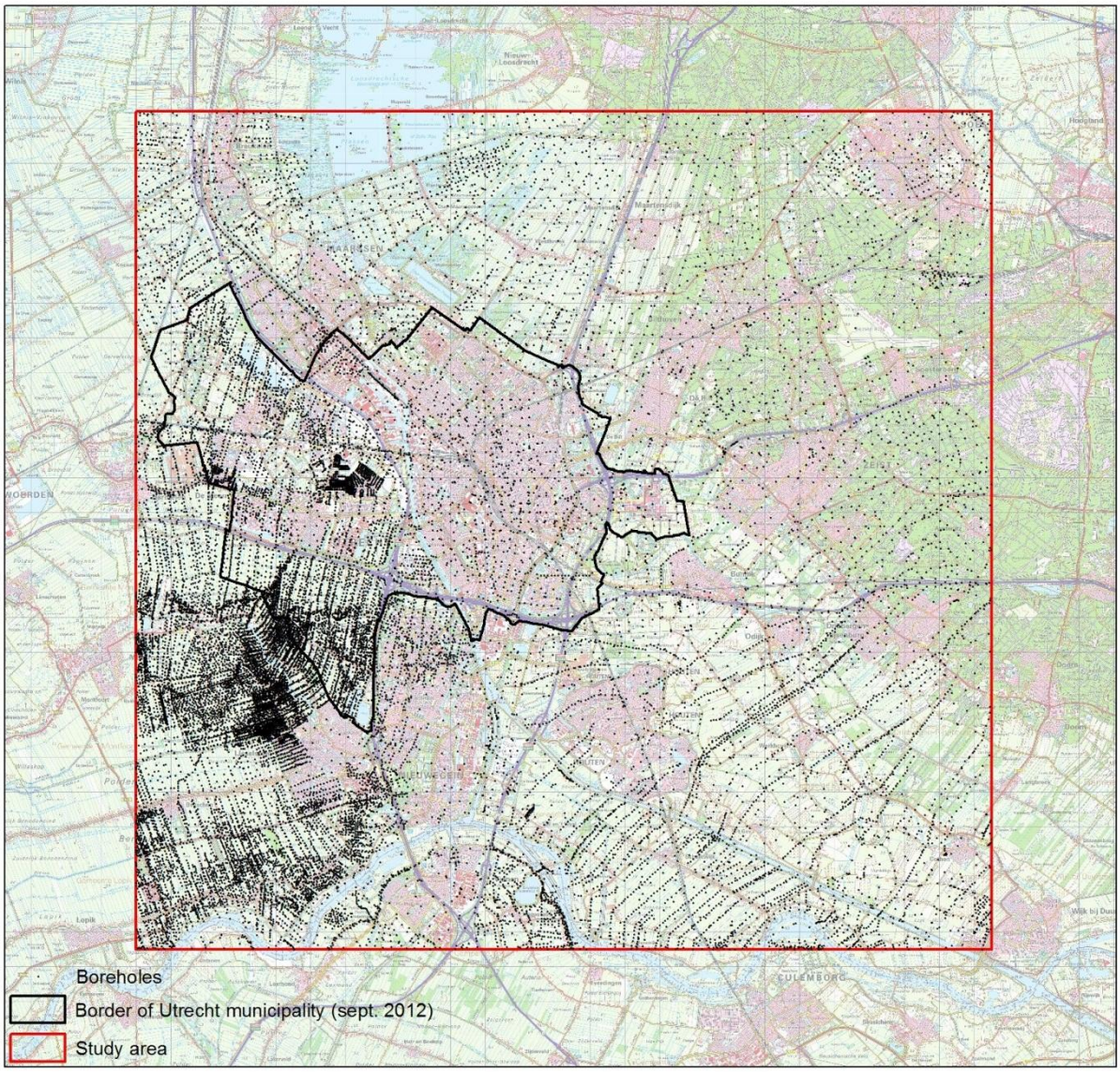

Figure A1 Location of the study area and the boreholes used

Although the number of data points has increased with regard to the GeoTOP Rivierengebied study, this number was not enough to decrease the cell size. Therefore this study has the same cell size as in GeoTOP Rivierengebied, being 100 by 100 m in 2D and 100 by 100 by 0.5 m in 3D.

Furthermore the latest version of the Digital Geological Model (DGM 2.2, including the latest fault data) has been used and an adjusted data quality criterion has been implemented.

The geological concept used in GeoTOP Rivierengebied still holds true for this study, therefore the distributional areas of all formations, layers and beds are kept the same as in GeoTOP Rivierengebied. These distributional areas and the boreholes itself form the input for the stratigraphic interpretation.

Stratigraphic interpretation

The boreholes have been interpreted automatically using in-house developed Python based scripts. The procedure included all criteria from GeoTOP Rivierengebied. The result of this step is a geologically interpreted data set (Figure A2), labeling top and base of formations, layers and beds in the boreholes. This information forms the input for the 2D layer modeling.

These automatically interpreted boreholes are checked using mapped transects from previous studies as well as new transects.

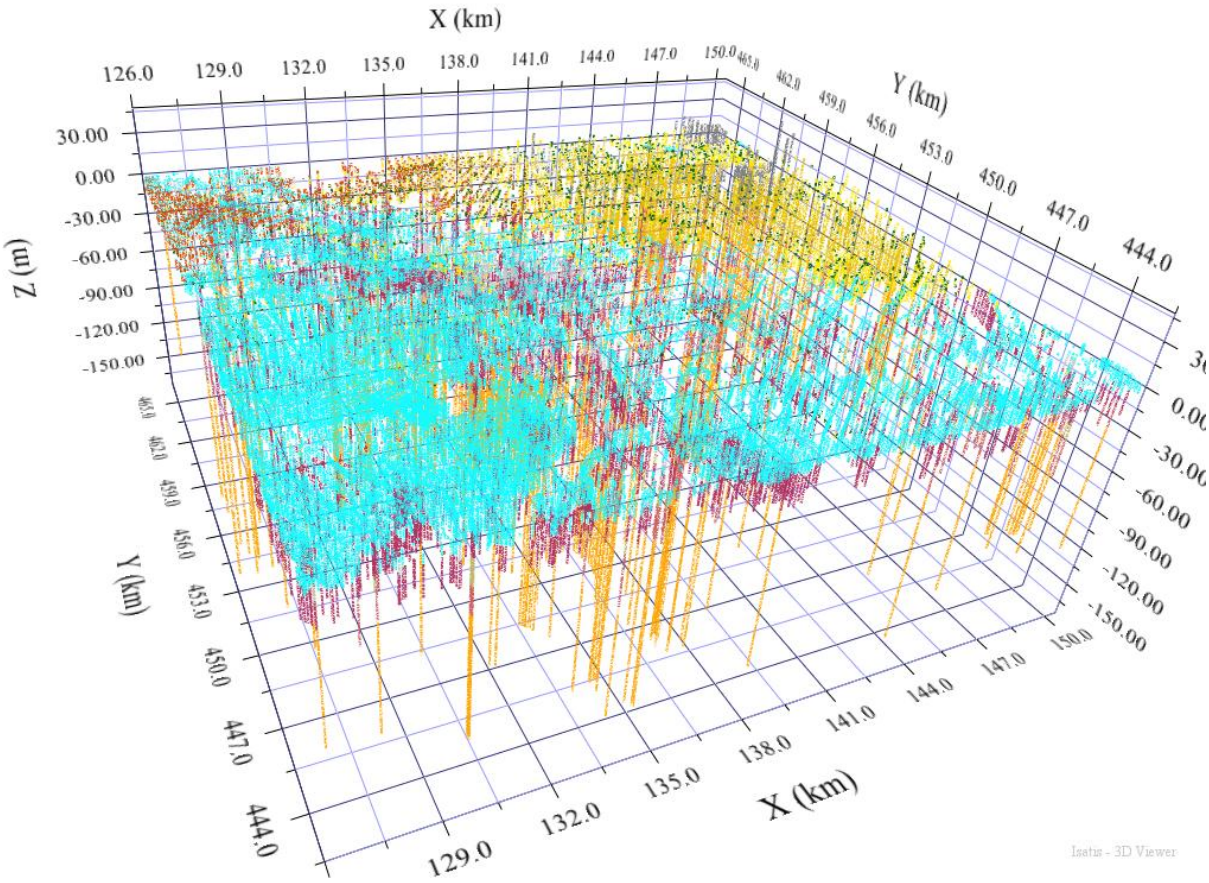

Figure A2 Stratigraphically interpreted boreholes in the study area, looked upon from the southwest. Colors indicate the difference units.

2D layer model

The next step is the construction of a geological 2D layer model for which the interpreted data set forms the basis. Using the same procedure as in GeoTOP Rivierengebied, layers representing the base of a geological unit are modeled. The two models can differ because of the extra data used and the use of the new version of DGM. DGM is used as a first approximation of the Pleistocene layers in the model to which new data is added. The Holocene units are modeled in more detail than in DGM, also modeling members and beds.

Additional to the geological units the channel belts of the rivers Rhine and Meuse are modeled separately (Berendsen, H.J.A. & Stouthamer, E., 2001). After consultation with Deltares and Gemeente Utrecht, the 2001 version of the channel belt map has been used in this study.

The interpolation procedure is a workflow consisting of several interpolation routines, mainly using Conditional Sequential Gaussian Simulation (SGS; Goovaerts, 1997; Chilès & Delfiner, 2012). This results in a geologically correct 2D layer model in which top and base of all geological units are modeled, including an estimate of their uncertainty.

This layer model is converted to a 3D voxel model, having voxels with a cell size of 100 by 100 by 0.5 m (Figure A3). This means that after this step every voxel has an estimate of its stratigraphy including an uncertainty.

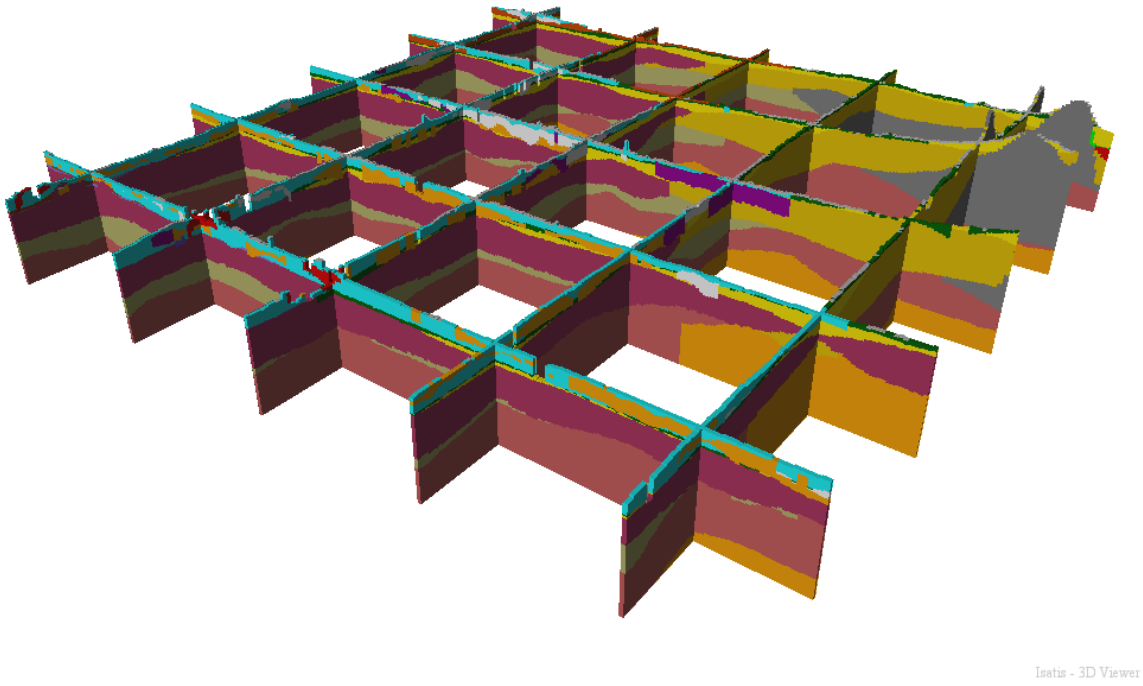

Figure A3 Fence diagram showing the modeled geological units in the study area, looked upon from the southeast. Note in the upper right corner the ice-pushed ridges in grey.

3D voxel model

The stratigraphic labeling of the voxels is used in the subsequent lithological modeling. For each stratigraphic unit this modeling is performed. As with the layer model, the (previous) channel belts of the Rhine and Meuse rivers are modeled as separate entities.

The lithological intervals in the boreholes are regularized to 0.5 m in order to give each interval the same weight in the interpolation procedure. This has only an effect on the intervals larger than 0.5 m, intervals less thick than 0.5 m keep their initial interval thickness. Furthermore all intervals are labeled with a lithoclass based on their descriptions (Table A1).

Table A1. Lithoclasses in the boreholes based on REGIS II

Lithoclass	*Number*	*Abbreviation*	*Grain size median*
Organic matter	1	o	-
Clay	2	k	-
Clayey sand, sandy clay and loam	3	kz	-
Fine sand	5	zf	≥ 63 µm and < 150 µm
Medium sand	6	zm	≥ 150 µm and < 300 µm
Coarse sand	7	zg	≥ 300 µm and < 2 mm
Gravel	8	g	≥ 2 mm
Shells	9	sch	-
Sand, grain size median unknown	10	z	Unknown

The interpolation procedure is performed in two steps and uses Sequential Indicator Simulation (SIS; Goovaerts, 1997; Chilès & Delfiner, 2012) as interpolation method. This simulation technique results in statistically equi-probable lithoclass estimations.

The first step is to run 10 simulations that simulate the distribution sand versus non-sand. In the next step per simulated result all voxels with a sand estimate are selected. For these selected voxels again 10 simulations are performed using only those intervals with known sand median grain size. This gives a total of 10 times 10 is 100 realisations of median grain size classes. For the non-sand voxels also 10 simulations are performed, simulating organic matter, clay and clayey sand/sandy clay.

As a result, all voxels have a lithoclass estimation, next to a stratigraphic estimation, as shown in Table A2 and illustrated in Figure A4.

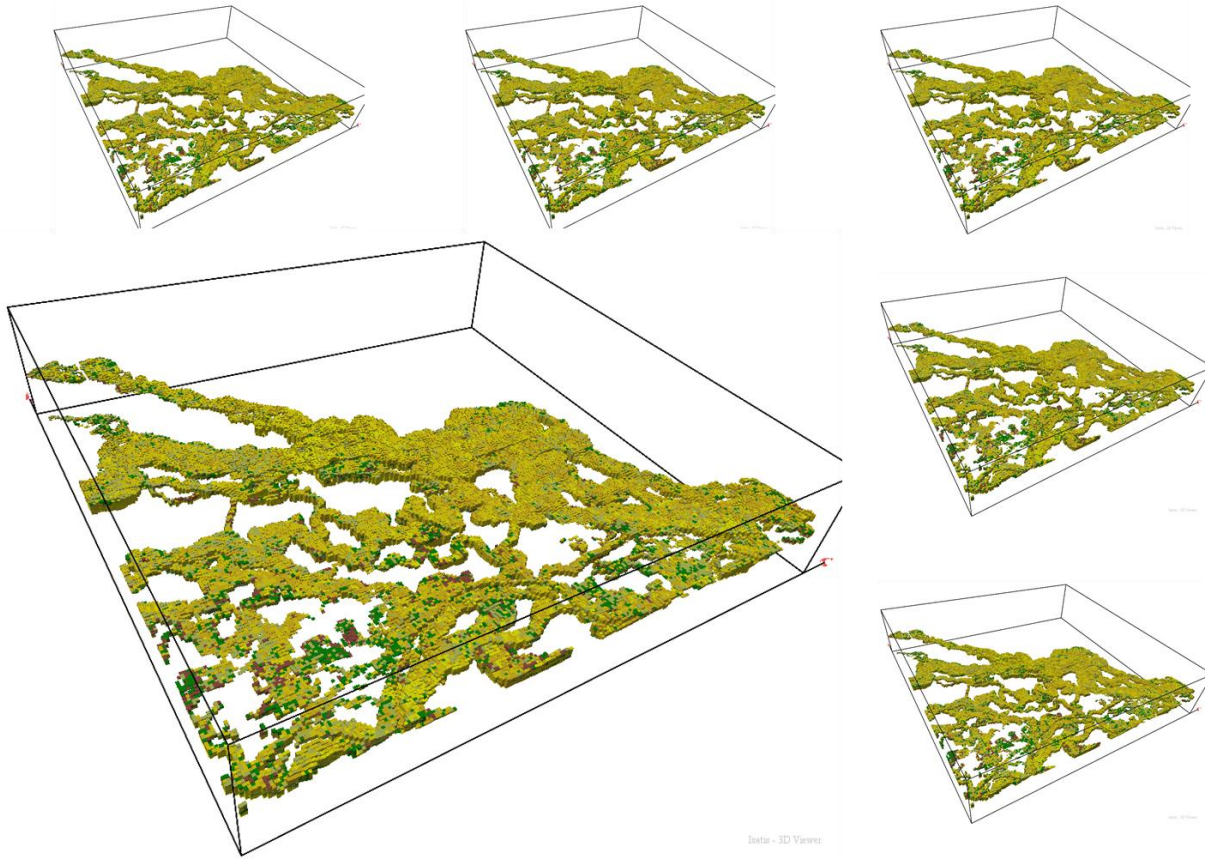

Figure A4. Six equi-probable realisations of lithoclasses within the channel belts are shown, looked upon from the southwest. Yellow colors indicate sand, green colors indicate clay and brown colors indicate peat

Table A2. Lithoclasses in the 3D voxel model based on REGIS II

Lithoclass	*Number*	*Abbreviation*	*Grain size median*
Anthropogenic deposits	0	a	-
Organic matter	1	o	-
Clay	2	k	-
Clayey sand, sandy clay and loam	3	kz	-
Fine sand	5	zf	≥ 63 µm and < 150 µm
Medium sand	6	zm	≥ 150 µm and < 300 µm
Coarse sand	7	zg	≥ 300 µm and < 2 mm
Gravel	8	g	≥ 2 mm
Shells	9	sch	

Parameterization

The result of the 3D modeling step are 100 realisations of lithoclass distributions. These realisations are parameterized, using their estimated stratigraphy and estimated lithoclass, with horizontal and vertical hydraulic conductivities. These conductivities are based on REGIS II (Annex I).

Quality control

In all previous described workflow steps quality control has taken place. Results are for example checked on their geological and statistical accuracy and plausibility.

Appendix A: Annex I

Stratigraphical name	Unit number	Lithoclass name	Lithoclass number	Kh (m/d)	Kv (m/d)
AAOP	1000	Antropogeen	0	5	5
NAWA	1050	Organisch (veen)	1	0.25	0.25
NAWA	1050	Klei	2	3.49E-03	3.49E-03
NAWA	1050	Kleiig zand/zandige klei	3	5.25E-02	5.25E-02
NAWA	1050	Fijn zand	5	0.74	0.52
NAWA	1050	Medium zand	6	3.6894	2.58
NAWA	1050	Grof zand	7	24.2	17
NAWA	1050	Grind	8	85	85
OEC	1070	Organisch (veen)	1	0.049	0.049
OEC	1070	Klei	2	0.0046	0.0046
OEC	1070	Kleiig zand/zandige klei	3	0.04	0.04
OEC	1070	Fijn zand	5	4.4	4.4
OEC	1070	Medium zand	6	11.5	11.5
OEC	1070	Grof zand	7	29.5	29.5
OEC	1070	Grind	8	85	85
NIHO	1090	Organisch (veen)	1	0.25	0.25
NIHO	1090	Klei	2	0.00291	0.00291
NIHO	1090	Kleiig zand/zandige klei	3	0.0525	0.0525
NIHO	1090	Fijn zand	5	0.74	0.52
NIHO	1090	Medium zand	6	6.29	4.4
NIHO	1090	Grof zand	7	24.2	17
NIHO	1090	Grind	8	85	85
NAWO	1100	Organisch (veen)	1	0.049	0.049
NAWO	1100	Klei	2	0.00291	0.00291
NAWO	1100	Kleiig zand/zandige klei	3	0.0314	0.0314
NAWO	1100	Fijn zand	5	0.71	0.5
NAWO	1100	Medium zand	6	6.29	4.4
NAWO	1100	Grof zand	7	24.2	17
NAWO	1100	Grind	8	85	85
EC	2010	Organisch (veen)	1	0.049	0.049
EC	2010	Klei	2	0.0046	0.0046
EC	2010	Kleiig zand/zandige klei	3	0.04	0.04
EC	2010	Fijn zand	5	4.4	4.4
EC	2010	Medium zand	6	11.5	11.5
EC	2010	Grof zand	7	29.5	29.5
EC	2010	Grind	8	85	85

NIBA	1130	Organisch (veen)	1	0.0004	0.0004
NIBA	1130	Klei	2	0.0046	0.0046
NIBA	1130	Kleiig zand/zandige klei	3	0.0314	0.0314
NIBA	1130	Fijn zand	5	0.71	0.5
NIBA	1130	Medium zand	6	11.5	11.5
NIBA	1130	Grof zand	7	29.5	29.5
NIBA	1130	Grind	8	85	85
BXWISIKO	3030	Organisch (veen)	1	0.049	0.049
BXWISIKO	3030	Klei	2	0.0046	0.0046
BXWISIKO	3030	Kleiig zand/zandige klei	3	0.04	0.004
BXWISIKO	3030	Fijn zand	5	4.4	0.44
BXWISIKO	3030	Medium zand	6	16.2	3.2
BXWISIKO	3030	Grof zand	7	21.6	10.8
BXWISIKO	3030	Grind	8	85	85
BXSC	3050	Organisch (veen)	1	0.049	0.049
BXSC	3050	Klei	2	0.0046	0.0046
BXSC	3050	Kleiig zand/zandige klei	3	0.08	0.016
BXSC	3050	Fijn zand	5	4.4	0.44
BXSC	3050	Medium zand	6	16.2	3.2
BXSC	3050	Grof zand	7	21.6	10.8
BXSC	3050	Grind	8	21.6	10.8
BX	3100	Organisch (veen)	1	0.049	0.049
BX	3100	Klei	2	0.0046	0.0046
BX	3100	Kleiig zand/zandige klei	3	0.04	0.004
BX	3100	Fijn zand	5	4.4	0.44
BX	3100	Medium zand	6	16.2	3.2
BX	3100	Grof zand	7	21.6	10.8
BX	3100	Grind	8	85	85
KRWY	4000	Organisch (veen)	1	0.049	0.049
KRWY	4000	Klei	2	0.0046	0.0046
KRWY	4000	Kleiig zand/zandige klei	3	0.04	0.02
KRWY	4000	Fijn zand	5	4.4	4.4
KRWY	4000	Medium zand	6	13.2	13.2
KRWY	4000	Grof zand	7	58.8	58.8
KRWY	4000	Grind	8	85	85
KR	4010	Organisch (veen)	1	0.049	0.049
KR	4010	Klei	2	0.0046	0.0046
KR	4010	Kleiig zand/zandige klei	3	0.04	0.02
KR	4010	Fijn zand	5	4.4	2.2
KR	4010	Medium zand	6	13.2	13.2

KR	4010	Grof zand	7	58.8	58.8
KR	4010	Grind	8	85	85
WB	4100	Organisch (veen)	1	0.049	0.049
WB	4100	Klei	2	0.0046	0.0046
WB	4100	Kleiig zand/zandige klei	3	0.04	0.04
WB	4100	Fijn zand	5	4.4	4.4
WB	4100	Medium zand	6	16.2	16.2
WB	4100	Grof zand	7	21.6	21.6
WB	4100	Grind	8	85	85
EE	4110	Organisch (veen)	1	0.049	0.049
EE	4110	Klei	2	0.00349	0.00349
EE	4110	Kleiig zand/zandige klei	3	0.0525	0.0525
EE	4110	Fijn zand	5	0.74	0.52
EE	4110	Medium zand	6	12.44	8.7
EE	4110	Grof zand	7	24.2	17
EE	4110	Grind	8	85	85
BE	4080	Organisch (veen)	1	0.049	0.049
BE	4080	Klei	2	0.0046	0.0046
BE	4080	Kleiig zand/zandige klei	3	0.04	0.02
BE	4080	Fijn zand	5	4.4	2.2
BE	4080	Medium zand	6	13.2	13.2
BE	4080	Grof zand	7	58	58
BE	4080	Grind	8	170	170
DR	5000	Organisch (veen)	1	0.049	0.049
DR	5000	Klei	2	0.0046	0.0046
DR	5000	Kleiig zand/zandige klei	3	0.04	0.04
DR	5000	Fijn zand	5	4.4	4.4
DR	5000	Medium zand	6	13.2	13.2
DR	5000	Grof zand	7	34.1	34.1
DR	5000	Grind	8	85	85
DRGI	5010	Organisch (veen)	1	0.049	0.049
DRGI	5010	Klei	2	0.0432	0.0432
DRGI	5010	Kleiig zand/zandige klei	3	0.0432	0.0432
DRGI	5010	Fijn zand	5	4.4	4.4
DRGI	5010	Medium zand	6	13.2	13.2
DRGI	5010	Grof zand	7	34.1	34.1
DRGI	5010	Grind	8	85	85
GE (DT)	5020	Organisch (veen)	1	0.049	0.049
GE (DT)	5020	Klei	2	0.0046	0.0046
GE (DT)	5020	Kleiig zand/zandige klei	3	0.04	0.04

GE (DT)	5020	Fijn zand	5	4.4	4.4
GE (DT)	5020	Medium zand	6	13.2	13.2
GE (DT)	5020	Grof zand	7	34.1	34.1
GE (DT)	5020	Grind	8	85	85
UR	5060	Organisch (veen)	1	0.049	0.049
UR	5060	Klei	2	0.0046	0.0046
UR	5060	Kleiig zand/zandige klei	3	0.04	0.04
UR	5060	Fijn zand	5	4.4	4.4
UR	5060	Medium zand	6	13.2	13.2
UR	5060	Grof zand	7	34.1	34.1
UR	5060	Grind	8	85	85
ST	5070	Organisch (veen)	1	0.049	0.049
ST	5070	Klei	2	0.0046	0.0046
ST	5070	Kleiig zand/zandige klei	3	0.04	0.04
ST	5070	Fijn zand	5	4.4	4.4
ST	5070	Medium zand	6	20	20
ST	5070	Grof zand	7	60	60
ST	5070	Grind	8	85	85
SY	5090	Organisch (veen)	1	0.049	0.049
SY	5090	Klei	2	0.046	0.0046
SY	5090	Kleiig zand/zandige klei	3	0.4	0.04
SY	5090	Fijn zand	5	4.4	0.44
SY	5090	Medium zand	6	13.2	1.32
SY	5090	Grof zand	7	34.1	34.1
SY	5090	Grind	8	85	85
AP	5080	Organisch (veen)	1	0.049	0.049
AP	5080	Klei	2	0.0046	0.0046
AP	5080	Kleiig zand/zandige klei	3	0.04	0.04
AP	5080	Fijn zand	5	4.4	4.4
AP	5080	Medium zand	6	13.2	13.2
AP	5080	Grof zand	7	58.8	58.8
AP	5080	Grind	8	85	85
PZWA (WA)	5120	Organisch (veen)	1	0.049	0.049
PZWA (WA)	5120	Klei	2	0.0015	0.0015
PZWA (WA)	5120	Kleiig zand/zandige klei	3	0.04	0.04
PZWA (WA)	5120	Fijn zand	5	4.4	4.4
PZWA (WA)	5120	Medium zand	6	13.2	13.2
PZWA (WA)	5120	Grof zand	7	34.1	34.1
PZWA (WA)	5120	Grind	8	125	125
MS	5130	Organisch (veen)	1	0.0004	0.0004

MS	5130	Klei	2	0.0029	0.0029
MS	5130	Kleiig zand/zandige klei	3	0.031	0.031
MS	5130	Fijn zand	5	0.74	0.52
MS	5130	Medium zand	6	12.44	8.7
MS	5130	Grof zand	7	24.2	17
MS	5130	Grind	8	85	85
KI	5140	Organisch (veen)	1	0.0002	0.0002
KI	5140	Klei	2	0.0002	0.0002
KI	5140	Kleiig zand/zandige klei	3	0.04	0.004
KI	5140	Fijn zand	5	4.4	0.88
KI	5140	Medium zand	6	13.2	2.64
KI	5140	Grof zand	7	45	22.5
KI	5140	Grind	8	85	85
OO	5150	Organisch (veen)	1	0.0004	0.0004
OO	5150	Klei	2	0.0022	0.0022
OO	5150	Kleiig zand/zandige klei	3	0.057	0.057
OO	5150	Fijn zand	5	0.74	0.52
OO	5150	Medium zand	6	12.44	8.7
OO	5150	Grof zand	7	24.2	17
OO	5150	Grind	8	85	85
BR	5180	Organisch (veen)	1	1.94E-10	1.94E-10
BR	5180	Klei	2	0.0029	0.0029
BR	5180	Kleiig zand/zandige klei	3	0.36	0.036
BR	5180	Fijn zand	5	2.4	0.48
BR	5180	Medium zand	6	12.43	8.7
BR	5180	Grof zand	7	24.2	17
BR	5180	Grind	8	85	85
AEC	6000	Organisch (veen)	1	0.049	0.049
AEC	6000	Klei	2	0.0046	0.0046
AEC	6000	Kleiig zand/zandige klei	3	0.04	0.04
AEC	6000	Fijn zand	5	4.4	4.4
AEC	6000	Medium zand	6	11.5	11.5
AEC	6000	Grof zand	7	29.5	29.5
AEC	6000	Grind	8	85	85
ANAWA	6010	Organisch (veen)	1	0.25	0.25
ANAWA	6010	Klei	2	3.49E-03	3.49E-03
ANAWA	6010	Kleiig zand/zandige klei	3	5.25E-02	5.25E-02
ANAWA	6010	Fijn zand	5	0.74	0.52
ANAWA	6010	Medium zand	6	3.6894	2.58
ANAWA	6010	Grof zand	7	24.2	17

ANAWA	6010	Grind	8	85	85
ANAWO	6020	Organisch (veen)	1	0.049	0.049
ANAWO	6020	Klei	2	0.00291	0.00291
ANAWO	6020	Kleiig zand/zandige klei	3	0.0314	0.0314
ANAWO	6020	Fijn zand	5	0.71	0.5
ANAWO	6020	Medium zand	6	6.29	4.4
ANAWO	6020	Grof zand	7	24.2	17
ANAWO	6020	Grind	8	85	85
BEC	6100	Organisch (veen)	1	0.049	0.049
BEC	6100	Klei	2	0.0046	0.0046
BEC	6100	Kleiig zand/zandige klei	3	0.04	0.04
BEC	6100	Fijn zand	5	4.4	4.4
BEC	6100	Medium zand	6	11.5	11.5
BEC	6100	Grof zand	7	29.5	29.5
BEC	6100	Grind	8	85	85
BNAWA	6110	Organisch (veen)	1	0.25	0.25
BNAWA	6110	Klei	2	3.49E-03	3.49E-03
BNAWA	6110	Kleiig zand/zandige klei	3	5.25E-02	5.25E-02
BNAWA	6110	Fijn zand	5	0.74	0.52
BNAWA	6110	Medium zand	6	3.6894	2.58
BNAWA	6110	Grof zand	7	24.2	17
BNAWA	6110	Grind	8	85	85
BNAWO	6120	Organisch (veen)	1	0.049	0.049
BNAWO	6120	Klei	2	0.00291	0.00291
BNAWO	6120	Kleiig zand/zandige klei	3	0.0314	0.0314
BNAWO	6120	Fijn zand	5	0.71	0.5
BNAWO	6120	Medium zand	6	6.29	4.4
BNAWO	6120	Grof zand	7	24.2	17
BNAWO	6120	Grind	8	85	85
CEC	6200	Organisch (veen)	1	0.049	0.049
CEC	6200	Klei	2	0.0046	0.0046
CEC	6200	Kleiig zand/zandige klei	3	0.04	0.04
CEC	6200	Fijn zand	5	4.4	4.4
CEC	6200	Medium zand	6	11.5	11.5
CEC	6200	Grof zand	7	29.5	29.5
CEC	6200	Grind	8	85	85
CNAWA	6210	Organisch (veen)	1	0.25	0.25
CNAWA	6210	Klei	2	3.49E-03	3.49E-03
CNAWA	6210	Kleiig zand/zandige klei	3	5.25E-02	5.25E-02
CNAWA	6210	Fijn zand	5	0.74	0.52

CNAWA	6210	Medium zand	6	3.6894	2.58
CNAWA	6210	Grof zand	7	24.2	17
CNAWA	6210	Grind	8	85	85
CNAWO	6220	Organisch (veen)	1	0.049	0.049
CNAWO	6220	Klei	2	0.00291	0.00291
CNAWO	6220	Kleiig zand/zandige klei	3	0.0314	0.0314
CNAWO	6220	Fijn zand	5	0.71	0.5
CNAWO	6220	Medium zand	6	6.29	4.4
CNAWO	6220	Grof zand	7	24.2	17
CNAWO	6220	Grind	8	85	85
DEC	6300	Organisch (veen)	1	0.049	0.049
DEC	6300	Klei	2	0.0046	0.0046
DEC	6300	Kleiig zand/zandige klei	3	0.04	0.04
DEC	6300	Fijn zand	5	4.4	4.4
DEC	6300	Medium zand	6	11.5	11.5
DEC	6300	Grof zand	7	29.5	29.5
DEC	6300	Grind	8	85	85
DNAWA	6310	Organisch (veen)	1	0.25	0.25
DNAWA	6310	Klei	2	3.49E-03	3.49E-03
DNAWA	6310	Kleiig zand/zandige klei	3	5.25E-02	5.25E-02
DNAWA	6310	Fijn zand	5	0.74	0.52
DNAWA	6310	Medium zand	6	3.6894	2.58
DNAWA	6310	Grof zand	7	24.2	17
DNAWA	6310	Grind	8	85	85
DNAWO	6320	Organisch (veen)	1	0.049	0.049
DNAWO	6320	Klei	2	0.00291	0.00291
DNAWO	6320	Kleiig zand/zandige klei	3	0.0314	0.0314
DNAWO	6320	Fijn zand	5	0.71	0.5
DNAWO	6320	Medium zand	6	6.29	4.4
DNAWO	6320	Grof zand	7	24.2	17
DNAWO	6320	Grind	8	85	85
EEC	6400	Organisch (veen)	1	0.049	0.049
EEC	6400	Klei	2	0.0046	0.0046
EEC	6400	Kleiig zand/zandige klei	3	0.04	0.04
EEC	6400	Fijn zand	5	4.4	4.4
EEC	6400	Medium zand	6	11.5	11.5
EEC	6400	Grof zand	7	29.5	29.5
EEC	6400	Grind	8	85	85
ENAWA	6410	Organisch (veen)	1	0.25	0.25
ENAWA	6410	Klei	2	3.49E-03	3.49E-03

ENAWA	6410	Kleiig zand/zandige klei	3	5.25E-02	5.25E-02
ENAWA	6410	Fijn zand	5	0.74	0.52
ENAWA	6410	Medium zand	6	3.6894	2.58
ENAWA	6410	Grof zand	7	24.2	17
ENAWA	6410	Grind	8	85	85
ENAWO	6420	Organisch (veen)	1	0.049	0.049
ENAWO	6420	Klei	2	0.00291	0.00291
ENAWO	6420	Kleiig zand/zandige klei	3	0.0314	0.0314
ENAWO	6420	Fijn zand	5	0.71	0.5
ENAWO	6420	Medium zand	6	6.29	4.4
ENAWO	6420	Grof zand	7	24.2	17
ENAWO	6420	Grind	8	85	85

APPENDIX B Model results at various time steps

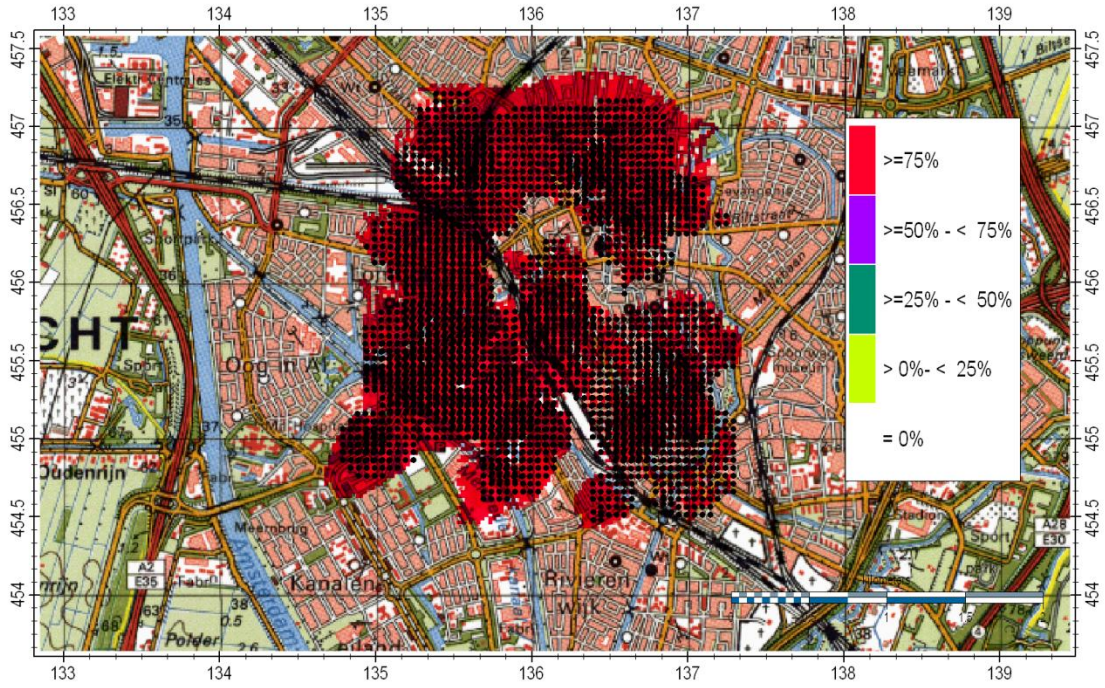

Figure B1 Top view with probability if the norm is violated for at least one component at 1-1 2018; black dots denote initial plumes

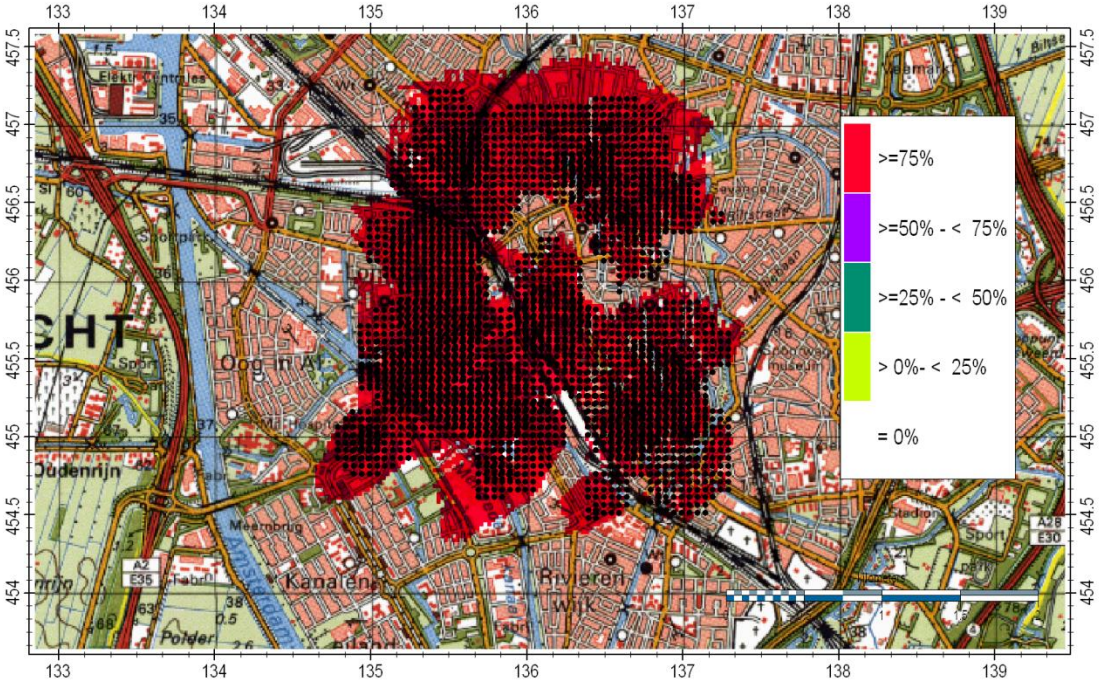

Figure B2 Top view with probability if the norm is violated for at least one component at 1-1 2023; black dots denote initial plumes

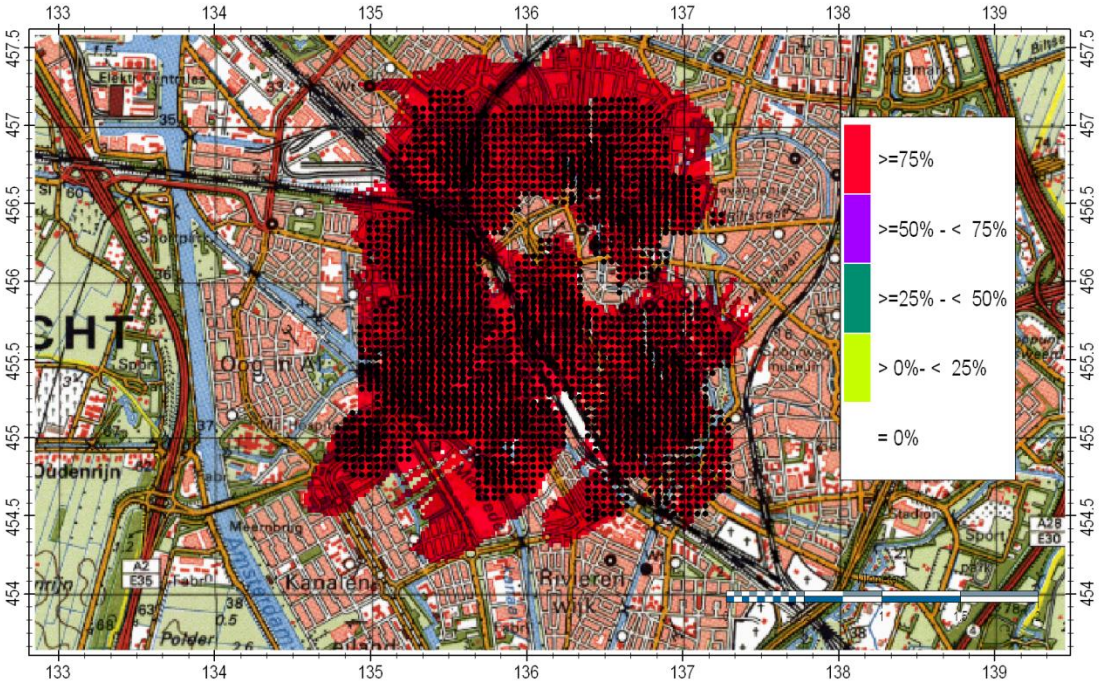

Figure B3 Top view with probability if the norm is violated for at least one component at 1-1 2033; black dots denote initial plumes

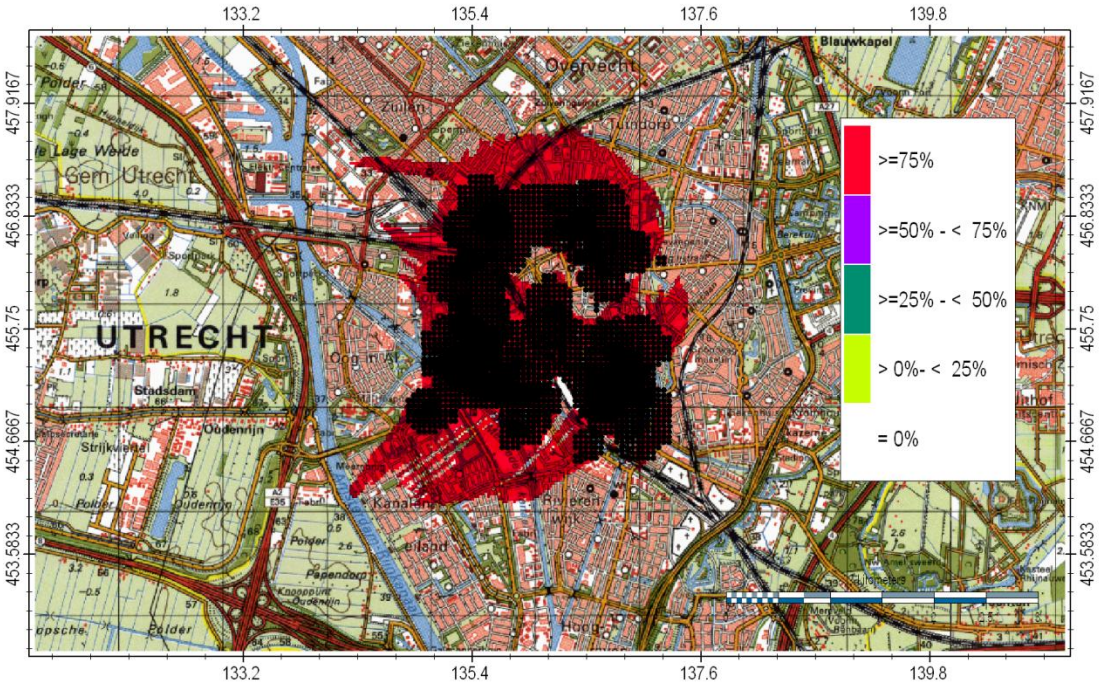

Figure B4 Top view with probability if the norm is violated for at least one component at 1-1 2063; black dots denote initial plumes

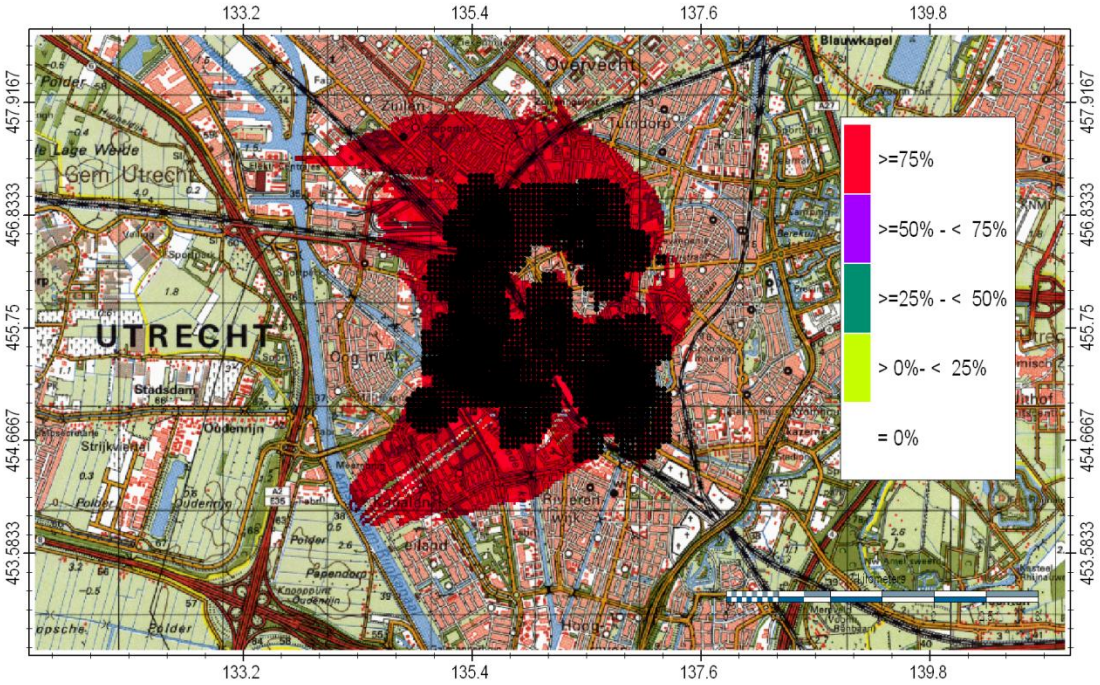

Figure B5 Top view with probability if the norm is violated for at least one component at 1-1 2113; black dots denote initial plumes

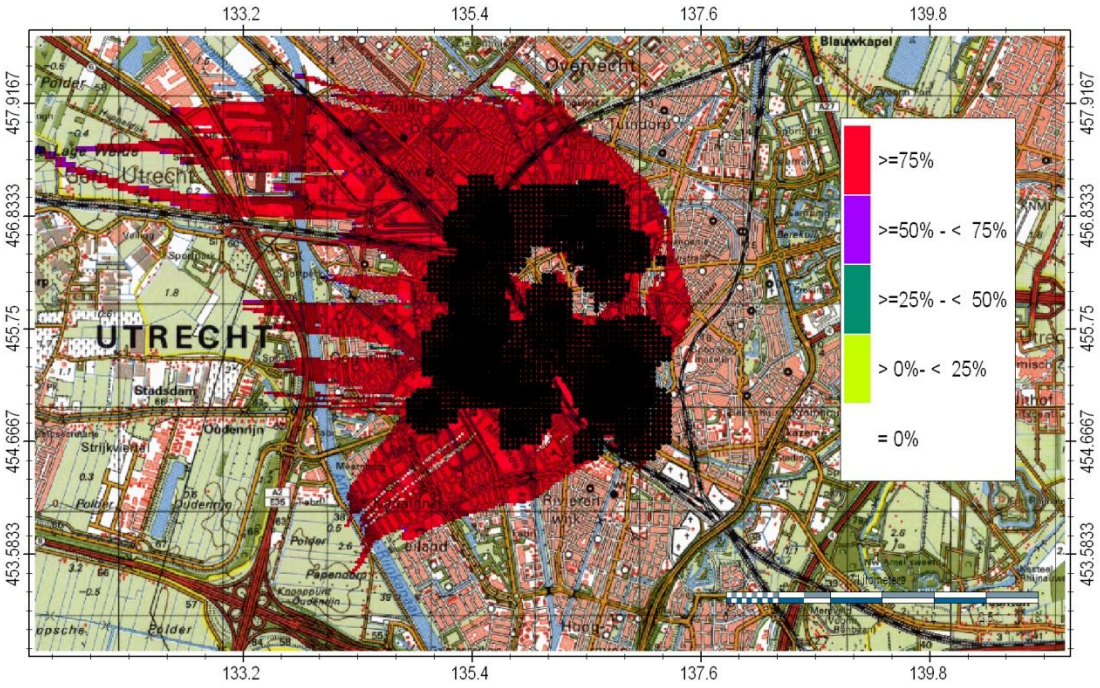

Figure B6 Top view with probability if the norm is violated for at least one component at 1-1 2213; black dots denote initial plumes

Document description

Title: Geohydrological modelling - Predictions for an area-oriented approach for groundwater contamination in the City of Utrecht.

Deposit number: -

Number of Pages: 44

Editor: J. Valstar, D. Maljers

Date of publication: April 4 2013

Contact: J. Valstar

Key words: area-oriented approach, groundwater reactive transport model

Translations:

Summary: A geohydrological model has been developed in order to predict the behaviour of a number of plumes with chlorinated hydrocarbons in the city of Utrecht. The model is set up to support the area-oriented approach for groundwater contamination.

Investing in Opportunities

This project has received European Regional Development Funding through INTERREG IV B.

INTERREG IVB